Available online at www.sciencedirect.com
ScienceDirect
Carbohydrate Research 341 (2006) 2927–2945
Carbohydrate RESEARCH

Conformational analysis of methyl 5-*O*-methyl septanosides: effect of glycosylation on conformer populations

Matthew P. DeMatteo,[a] Song Mei,[b] Ryan Fenton,[b] Martha Morton,[b] Donna M. Baldisseri,[c] Christopher M. Hadad[a,*] and Mark W. Peczuh[b,*]

[a]*Department of Chemistry, The Ohio State University, 100 West 18th Avenue, Columbus, OH 43210, USA*
[b]*Department of Chemistry, The University of Connecticut, 55 North Eagleville Road, Storrs, CT 06269, USA*
[c]*BrükerBioSpin Corp., 15 Fortune Drive, Manning Park, Billerica, MA 01821, USA*

Received 16 August 2006; received in revised form 15 September 2006; accepted 28 September 2006
Available online 4 October 2006

Abstract—Methyl 5-*O*-methyl-α-D-*glycero*-D-idoseptanoside (**3**) and methyl 5-*O*-methyl-β-D-*glycero*-D-guloseptanoside (**4**) were investigated as (1→5)-linked di-/oligoseptanoside mimetics. Here we report the synthesis of **3** and **4** and describe their preferred solution conformations through a combination of ab initio/DFT calculations and ^{1}H $^{3}J_{H,H}$ NMR coupling constant analysis. The conformations of **3** and **4** observed in this study are discussed in comparison to those of the parent (C5 hydroxy) compounds **1** and **2**. The results indicate that methyl 5-*O*-methyl-α-septanoside **3** is relatively rigid and adopts the same $^{3,4}TC_{5,6}$ conformation as **1**. Methyl 5-*O*-methyl-β-septanoside **4** is somewhat less rigid than its parent septanoside (**2**). In addition to the $^{6,O}TC_{4,5}$ conformation adopted by **2**, β-septanoside **4** also populates the adjacent $^{3,4}TC_{5,6}$ conformation. Glycosylation at C5 on β-septanoside **4** therefore increases its overall flexibility and allows access to alternative ring conformations.

Keywords: Septanose carbohydrate; Conformational analysis

1. Introduction

Septanoses[1] are analogs of natural carbohydrates characterized by having a seven-membered ring rather than the five- or six-membered rings of furanoses and pyranoses, respectively. Although limited, the biological and biophysical activities of the reported septanose carbohydrates indicate that these structures may be useful probes for glycobiology.[2,3] Structurally related polyhydroxyazepanes are known to be inhibitors of glycosidase and protease enzymes.[4] In each of these cases, the low energy conformations of the specific seven-membered rings were used to explain the reported activities. An understanding of the conformational preferences of these highly functionalized seven-membered rings is, however, incomplete. In fact, one question that remains to be clearly addressed is whether or not septanoses and related rings are inherently flexible. That is, are there several low energy conformers available to a given septanose, and are the barriers to interconversion between them relatively low? If multiple conformations of similar energies are available to a given structure, then it may be expected to populate each of them and therefore be considered flexible.[5]

Other computational and spectroscopic investigations of monocyclic seven-membered ring systems (cycloheptane, oxepane as well as 1,3- and 1,4-dioxepane) have established some fundamental principles concerning conformation.[6–9] First, of the twist-chair (TC), chair (C), twist-boat (TB), and boat (B) conformations, the TC is nearly always the global low energy minimum. For the seven-membered rings of low symmetry, individual unique conformers are defined by adding super- and subscripts to the TC/C descriptors. For TC conformers, three atoms define a molecular plane. Atoms above this plane are superscript and atoms below the plane are

* Corresponding authors. E-mail addresses: hadad.1@osu.edu; mark.peczuh@uconn.edu

0008-6215/$ - see front matter © 2006 Elsevier Ltd. All rights reserved.
doi:10.1016/j.carres.2006.09.024

subscript. This is similar for the C conformers, but in this case, four atoms define the molecular plane. Second, the TC and C conformers may interconvert via pseudorotation, as can the TB and B conformers. The TB/B equilibrium is often higher in energy and not populated. Third, the pathways for interconversion between individual TC and C conformers are expected to be complex. The interconversions would necessarily be defined by a four-dimensional surface as furanose interconversions are described by a wheel (two-dimensional) and pyranose interconversions by a sphere (three-dimensional).[10] Nonetheless, a given C conformer may be considered as a transition state between two (relatively) low energy TC conformers.[11] Prior studies have shown that factors such as sterics, hydrogen bonding, and electronic effects are important for determining the preferred low energy conformations.

We previously reported on the conformational analysis of two methyl septanosides, methyl α-D-*glycero*-D-idoseptanoside (**1**), and methyl β-D-*glycero*-D-guloseptanoside (**2**) (Chart 1).[7] Our approach was based on the method originally developed on methyl α-D-arabinofuranoside.[12] Briefly, a family of starting conformers were generated by a Monte Carlo search followed by AMBER minimization. Low energy conformers within 3–5 kcal/mol of the global minimum were then evaluated using HF and B3LYP density functional theory (DFT) calculations to generate a Boltzmann distribution of conformers based on their relative energies. The low energy conformers that contributed to the Boltzmann were also used in DFT calculations to give predicted $^{3}J_{H,H}$ and $^{1}J_{C,H}$ coupling constants. These values were then compared to experimental values obtained by NMR spectroscopy. Key observations made in the original study were (i) for each methyl septanoside, one ring conformer was preferred over all others with nearby conformers being 2–5 kcal/mol higher in energy; (ii) the low energy conformations were twist-chair (TC) conformers; (iii) the calculated $^{3}J_{H,H}$ values derived from minimized structures when compared to the ^{1}H NMR data were sufficient to assign the α- and β-anomeric structures; (iv) the anomeric effect contributed to the preferred conformation of α-septanoside **1**, but was not operative in forcing the aglycon methyl group in **2** into a pseudo-axial orientation. Overall, the initial exercise proved that to be a valuable tool in determining the preferred, low-energy conformations of methyl septanosides in general.

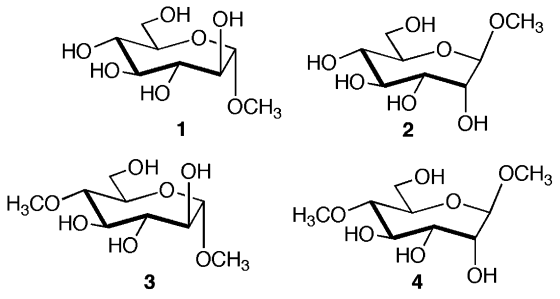

Chart 1.

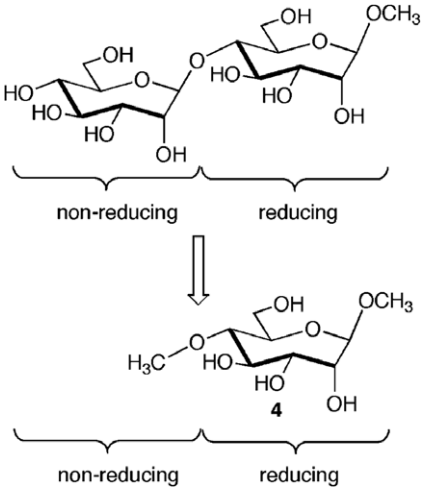

Figure 1. Methyl 5-*O*-methyl-β-D-*glycero*-D-guloseptanoside (**4**) as a model for the reducing end residue of a β-linked diseptanoside.

Here we report the synthesis and conformational analysis of two new methyl septanosides, methyl 5-*O*-methyl-α-D-*glycero*-D-idoseptanoside (**3**) and methyl 5-*O*-methyl-β-D-*glycero*-D-guloseptanoside (**4**). These 5-*O*-methyl septanosides serve as models for the reducing end sugar of di- and oligoseptanosides (Fig. 1). This is the first detailed effort toward the conformational analysis of models of diseptanosides. The methyl group is a surrogate for the residue at the non-reducing end of the di- or oligoseptanoside, and it also simplifies the computational and spectroscopic efforts. While a methyl group is perhaps a small surrogate for an oligosaccharide linked via a glycosidic bond, some prior reports with furanosides suggest that this model can provide a great insight.[14] Indeed, we were interested in determining if glycosylation at C5 of septanoses **1** and **2** would change the distribution of their preferred conformers as has been observed in other carbohydrate systems.[12] Defining diseptanoside structures that contain either an α-(1→5)-linkage or a β-(1→5)-linkage are valuable to us because they approximate the natural disaccharides maltose and cellobiose.[13] Repetition of these diseptanoside structural units should give insight into the shapes and superstructures of the corresponding polyseptanosides.

2. Results and discussion

2.1. Synthesis of methyl septanosides (3) and (4)

We considered two complementary routes for the synthesis of target methyl septanosides **3** and **4**. They

differed by where the regioselective opening of a benzylidene protecting group and the subsequent methylation of the exposed hydroxyl would be staged in the overall sequence. One option would have opened the 5,7-*O*-benzylidene of a methyl septanoside followed by the O5 methylation. This route was ruled out because the epoxidation and methanolysis reactions on the parent oxepine (**5**) were quite selective, yielding only the methyl β-septanoside[14] and we were interested in both the α- and the β-septanoside diastereomers in this systems. We therefore opted for a second route where oxepine **6** would undergo epoxidation and methanolysis in analogy to the synthesis of the parent compounds[7] (**1** and **2**) starting from **7**. Based on the earlier results with **7**, we anticipated that **6** would give access to both anomers (α/β) of the product methyl septanosides.

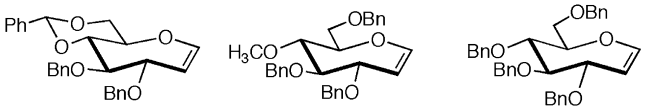

5 **6** **7**

The preparation of 5-*O*-methyl oxepine **6** is shown in Scheme 1. The known lactol **8**, prepared in five steps from methyl α-D-glucopyranoside, served as the starting material for the sequence.[15] The treatment of **8** with *n*-butyllithium and addition of this material into a solution of methylene triphenylphosphane in THF provided heptenitol **9** (64%). The newly exposed hydroxyl group was then converted to the vinyl ether using $Pd(OAc)_2$ and 1,10-phenanthroline in ethyl vinyl ether to give **10** in an 80% yield. Ring-closing metathesis of diene **10** using Schrock's catalyst in toluene provided oxepine **6** (89%).[16]

Methyl septanosides **3** and **4** were prepared from oxepine **6** under standard conditions (Scheme 2). The epoxidation of **6** using dimethyldioxirane (DMDO) in methylene chloride was followed by the epoxide opening of the intermediate 1,2-anhydroseptanose using sodium methoxide in methanol to give the protected methyl septanosides **11** and **12** in a 53% yield (1:2 α:β). Structures **11** and **12** were tentatively assigned based on the similarity of their elution profiles to the tetra-benzyl protected methyl septanosides during column chromatography. The benzyl protecting groups on **11** and **12** were then efficiently (>95% in each case) removed by hydrogenolysis to provide the α- and β-methyl 5-*O*-methyl septanosides **3** and **4**. The α:β selectivity observed in the epoxidation/methanolysis steps was nearly the same as that observed for oxepine **7**; this result was expected based on the fact that they differ only in the protecting group at the relatively remote (from the site of epoxidation) C5 position. A more detailed analysis of the anomers of the product methyl 5-*O*-methyl septanosides is provided below.

In conjunction with the experimental efforts, we utilized computational methods to understand the conformational flexibility in these systems, and compared theoretical NMR parameters directly to the experimentally determined values.

2.2. Monte Carlo and AMBER* results for 3

The Monte Carlo search for **3** resulted in 2979 unique conformations that covered a wide variety of internal dihedral angles for the septanose ring. This provides a good indication that the search was able to produce diverse coverage of the conformational space available to this structure.

An assignment of the conformation of the ring was made by visual inspection and quantitative evaluation of the appropriate endocyclic dihedral angles of the conformations within ~3.5 kcal/mol of the global minimum according to the AMBER* force field (see Supplementary data). Each conformer was given a unique number, starting from number 1 for the global minimum as

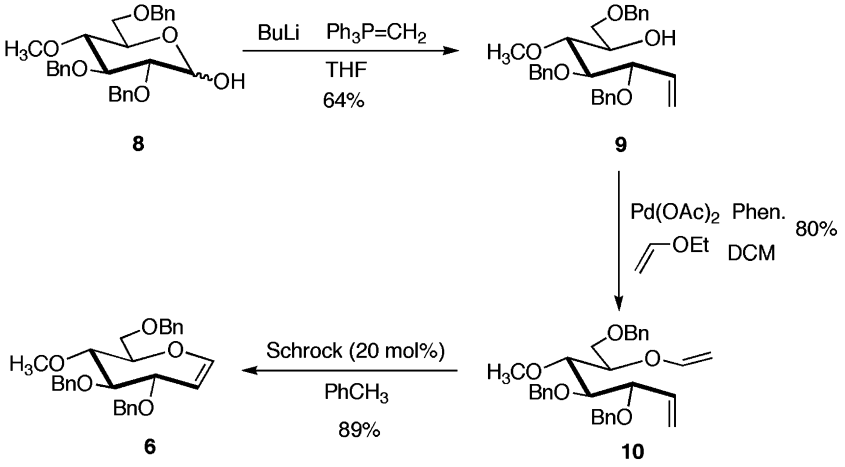

Scheme 1.

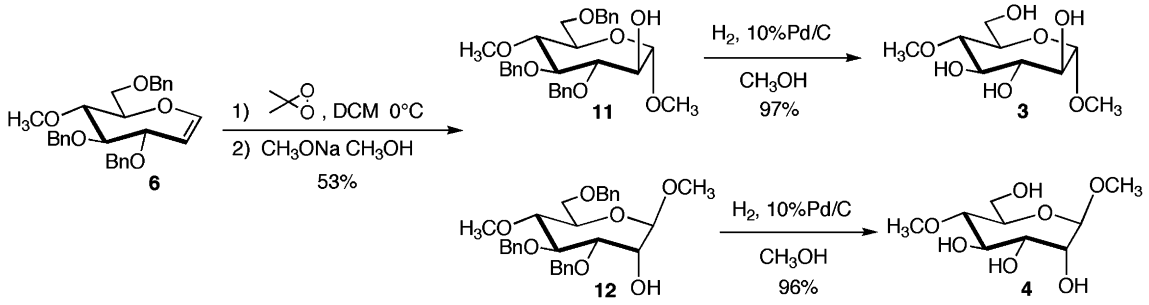

Scheme 2.

calculated by the AMBER* force field. It was noted that the majority of these low energy conformers consisted of septanose rings in the $^{3,4}TC_{5,6}$ conformation. This was the same conformation that structure **1** (Chart 1) was shown to adopt for its lowest energy conformers. The next most abundant conformation for the ring was the $^{1,2}TC_{3,4}$ conformation. Again, this was in accordance with our previous results for **1**. Other than these conformers, only a couple of other chair and twist-chair conformers were found to comprise the lowest energy conformers for **3**. It is worth noting that despite alkylation of the C5 hydroxyl group, there was still very little conformational flexibility for the septanose ring of **3**. The most significant difference observed between unique conformations is the orientation of the exocyclic hydroxyl and hydroxymethyl groups. Of particular note is the orientation about the C6–C7 bond. The AMBER* force field predicted that the global minimum would adopt a gt orientation about this bond.

It appears that the $^{3,4}TC_{5,6}$ conformation may be preferred as this conformation allows for a high degree of intramolecular hydrogen bonding to take place between the exocyclic hydroxyl groups. This hydrogen bonding appears to be favored despite the inclusion of the dielectric constant of water in the AMBER* calculations. (Tables of hydrogen-bonding distances are provided in the Supplementary data.)

2.3. Gas-phase HF/6-31G* results for 3

The conformations within ~3.5 kcal/mol of the global minimum according to the AMBER* force field were fully optimized at the HF/6-31G* level of theory (Table 1). It should be noted from these data that the HF/

Table 1. Calculated conformational distribution for the α-septanoside (**3**)[a]

Conformer #	AMBER* E_{rel}	HF/6-31G* E_{rel}	Boltzmann contribution[b] (%)	Ring conformation	C6–C7 rotamer[c]
6	0.19	0.00	69.29	$^{3,4}TC_{5,6}$	gg
10	0.86	0.61	24.54	$^{3,4}TC_{5,6}$	gg
1	0.00	1.84	3.11	$^{3,4}TC_{5,6}$	gt
15	1.00	2.71	0.71	$^{3,4}TC_{5,6}$	gt
2	0.02	2.85	0.56	$^{3,4}TC_{5,6}$	gt
126	3.01	3.04	0.41	$^{3,4}TC_{5,6}$	gt
131	3.06	3.13	0.35	$^{3,4}TC_{5,6}$	gg
42	1.94	3.15	0.34	$^{3,4}TC_{5,6}$	gt
48	2.11	3.61	0.16	$^{3,4}TC_{5,6}$	gg
91	2.71	3.68	0.14	$^{3,4}TC_{5,6}$	gg
71	2.47	3.73	0.13	$^{3,4}TC_{5,6}$	gg
13	0.91	4.02	0.08	$^{3,4}TC_{5,6}$	gt
25	1.25	4.51	0.03	$^{1,2}TC_{3,4}$	gg
66	2.39	4.65	0.03	$^{3,4}TC_{5,6}$	gg
22	1.16	4.73	0.02	$^{3,4}TC_{5,6}$	gt
81	2.58	4.86	0.02	$^{3,4}TC_{5,6}$	gg
45	2.06	4.90	0.02	$^{3,4}TC_{5,6}$	gg
109	2.88	4.94	0.02	$^{3,4}TC_{5,6}$	gg
54	2.20	5.20	0.01	$^{5}C_{1,2}$	gt
121	2.98	5.26	0.01	$^{3,4}TC_{5,6}$	gg
4	0.19	5.65	0.00	$^{1,2}TC_{3,4}$	gt
9	0.78	5.85	0.00	$^{1,2}TC_{3,4}$	gt
29	1.49	5.87	0.00	$^{3,4}TC_{5,6}$	gt

[a] Relative energies for each conformer, at each level of theory, are in kcal/mol.
[b] The Boltzmann contribution, as a percentage, is determined based on the relative energies calculated at the HF/6-31G* level of theory.
[c] From HF/6-31G* optimized geometries.

6-31G* level of theory predicted a different global minimum than that predicted by the AMBER* force field. This same tendency was previously observed in our studies of **1** and **2**. In this case, conformer 6 is the global minimum rather than 1. Once again, we examined whether the optimization at the HF/6-31G* level of theory severely altered the conformations from those determined using AMBER*. There was virtually no change in the geometries between the AMBER* and HF/6-31G* levels of theory. Rather, the nature of the difference between these two methods appears to be their treatment of important hydrogen-bonding interactions.

Comparison of the lowest energy conformations that contribute greater than 1% to the Boltzmann distribution is provided in Figure 2. The HF/6-31G* level of theory predicted that only three conformers contributed significantly to this distribution. The conformer predicted to be the global minimum at the AMBER* level was actually a much smaller contributor to the Boltzmann distribution at the HF/6-31G* level of theory. All of these low energy conformations had very similar geometries, occupying a $^{3,4}TC_{5,6}$ conformation for the ring with intramolecular hydrogen bonding among the exocyclic hydroxyl groups of the ring. The two largest contributors maintained a gg orientation for the C6–C7 dihedral angle. The global minimum (conformer 6) had its exocyclic hydroxyl groups oriented in a clockwise cyclic array such that each hydroxyl hydrogen was hydrogen-bonded to the next hydroxyl oxygen. An energetic preference for this conformation may arise from an

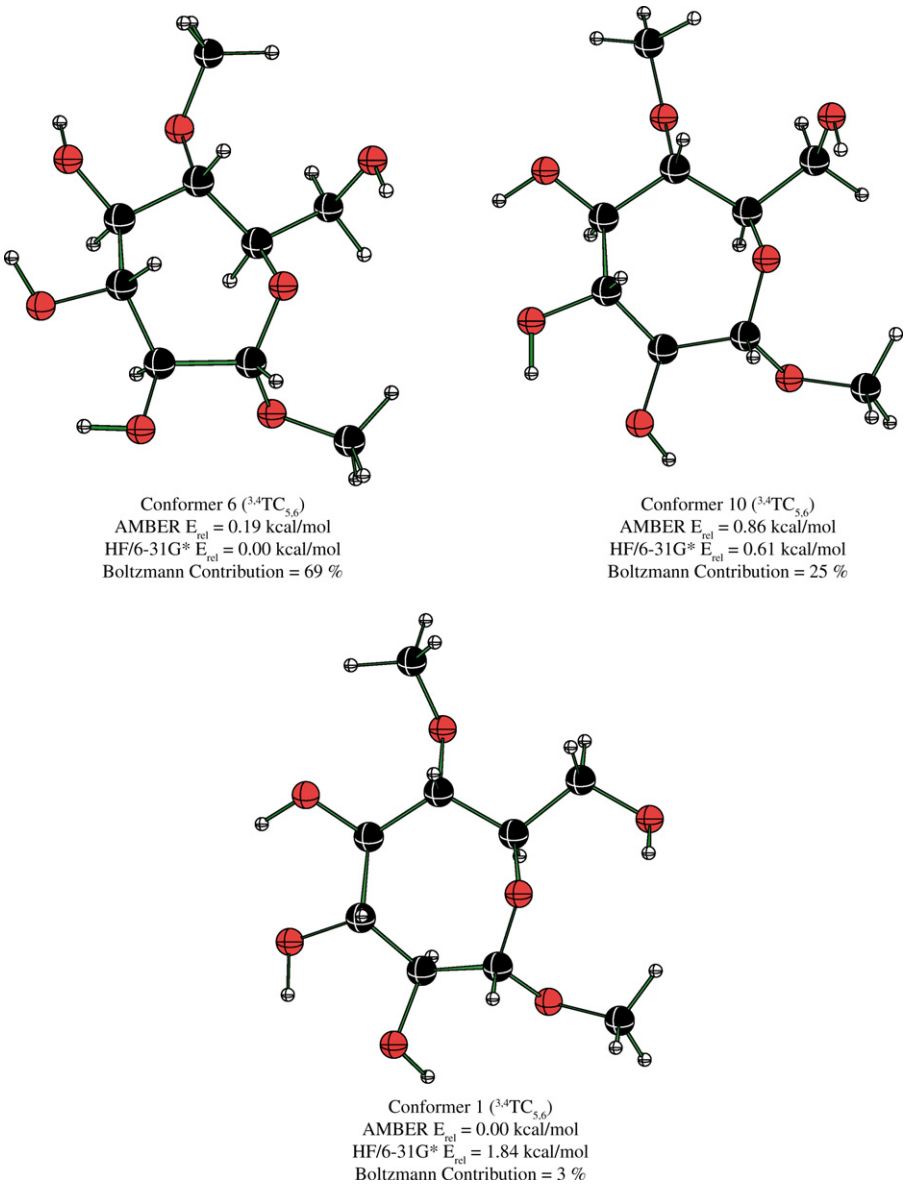

Figure 2. The lowest energy conformers of α anomer **3**. The conformer number, ring conformation, relative energies at the AMBER and HF/6-31G* levels of theory, as well as contribution to the HF/6-31G* Boltzmann distribution are also shown.

additional hydrogen bond that is possible with this configuration of the exocyclic hydroxyl groups that is not possible in the others. The only difference for the next energetic conformer (conformer 10) is that the hydrogen-bonding array is oriented in a counterclockwise fashion. Conformer 1 possessed much the same geometry as conformer 10 with the only notable exception being the orientation about the C6–C7 bond. Instead this group was oriented in a gt orientation. Clearly, the HF/6-31G* level has determined that a gt orientation is a less energetically favored conformation about the C6–C7 bond than the gg orientation.

The energetic trends determined by the HF/6-31G* level of theory predicted that the global minimum would comprise 69% of the Boltzmann distribution. Therefore, this conformer was predicted to be the most prevalent conformation for **3**. In fact, there was so little difference between the lowest energy conformations that the septanose ring essentially only adopts a $^{3,4}TC_{5,6}$ conformation with only minor variations in the exocyclic hydroxyl and hydroxymethyl groups.

2.4. Gas-phase and PCM B3LYP/6-311+G** single-point energy calculations for 3

Higher-level, single-point energy calculations were performed on the HF/6-31G* optimized conformers to determine whether there was a significant variation using other levels of theory. To this end, B3LYP/6-311+G**//HF/6-31G* level single-point energy calculations were performed and the results were compared to those obtained using the bottom-of-the-well energies from the HF/6-31G* calculations. As a second comparison to determine whether solvation might perturb the results, calculations were performed using the PCM B3LYP/6-311+G**//HF/6-31G* level of theory with methanol as the designated solvent. These series of single-point energy calculations provided results very similar to those obtained at the HF/6-31G* level of theory (Table 2). The only observed difference was that the higher levels of theory (particularly the PCM results) demonstrated a slightly larger sampling of the lowest energy conformations than those predicted by the gas-phase HF results. It was still predicted that the septanose ring would exclusively adopt a $^{3,4}TC_{5,6}$ conformation with the only variation being due to the orientation of the exocyclic hydroxyl and hydroxymethyl groups.

2.5. Monte Carlo and AMBER* results for 4

The Monte Carlo search for β-anomer **4** resulted in 1050 unique conformers within ~12 kcal/mol of the global minimum according to the AMBER* force field. These conformers covered a wide variety of internal dihedral angles for the septanose ring. As with α-anomer **3**, this

Table 2. Calculated conformational distribution for the α-septanoside (**3**)[a] as calculated at different levels of theory

Conformer #	AMBER* E_{rel}	HF/6-31G* E_{rel}	B3LYP/6-311+G** (gas phase) E_{rel}	PCM B3LYP/6-311+G** E_{rel}	HF/6-31G* Boltzmann contribution (%)	B3LYP/6-311+G** Boltzmann contribution (%)	PCM B3LYP/6-311+G** Boltzmann contribution (%)
6	0.19	0.00	0.00	0.00	69.29	67.82	17.58
10	0.86	0.61	0.70	0.07	24.54	20.85	16.85
1	0.00	1.84	1.54	1.46	3.11	5.05	1.60
15	1.00	2.71	2.28	0.19	0.71	1.45	10.88
2	0.02	2.85	2.33	2.41	0.56	1.32	0.33
126	3.01	3.04	2.44	0.67	0.41	1.11	4.34
131	3.06	3.13	2.95	3.03	0.35	0.46	0.19
42	1.94	3.15	3.04	4.59	0.34	0.40	0.01
48	2.11	3.61	3.26	0.66	0.16	0.28	9.52
91	2.71	3.68	3.41	0.95	0.14	0.22	4.40
71	2.47	3.73	3.39	1.13	0.13	0.22	2.78
13	0.91	4.02	3.53	0.73	0.08	0.18	3.30
25	1.25	4.51	4.04	2.97	0.03	0.07	0.15
66	2.39	4.65	3.88	0.81	0.03	0.10	7.71
22	1.16	4.73	3.98	1.19	0.02	0.08	2.11
81	2.58	4.86	4.66	1.72	0.02	0.03	0.85
45	2.06	4.90	3.91	3.35	0.02	0.09	0.06
109	2.88	4.94	4.72	1.67	0.02	0.02	0.84
54	2.20	5.20	3.93	3.76	0.01	0.09	0.02
121	2.98	5.26	4.61	1.36	0.01	0.03	3.00
4	0.19	5.65	4.71	3.93	0.00	0.02	0.03
9	0.78	5.85	4.90	2.43	0.00	0.02	0.31
29	1.49	5.87	5.01	2.16	0.00	0.01	0.44

[a] Relative energies for each conformer, at each level of theory, are in kcal/mol.

process provided a good coverage of the conformational space available to the septanose ring.

The conformation of the ring was assigned by visual inspection of the conformations within ~3.5 kcal/mol of the global minimum, as calculated by the AMBER* force field. Each conformer was given a unique number beginning with 1 for the global minimum according to this force field. Compared with **3**, there was considerable conformational diversity within the septanose ring of **4** (Table 3). In the lowest energy conformers according to the AMBER* force field, the ring adopted a $^{6,O}TC_{4,5}$ conformation. Several other chair and twist-chair conformations were located in the lowest energy structures including $^{5}C_{1,2}$, $^{3,4}TC_{5,6}$, $^{4,5}TC_{2,3}$, $^{3}C_{6,O}$, and $^{1,2}TC_{6,O}$. Overall, it would appear that the septanose ring of **4** was much more conformationally flexible than that of **3**. In all of the located conformations, the exocyclic hydroxyl groups preferred orientations that maximized intramolecular hydrogen bonding.

2.6. Gas-phase HF/6-31G* results for 4

Once again, all conformations within ~3.5 kcal/mol of the global minimum according to the AMBER* force field were fully optimized at the HF/6-31G* level of theory (Table 3). The global minimum according to the HF/6-31G* level of theory was noticeably different from that predicted by AMBER*. The global minimum predicted by HF/6-31G* was conformer 7 (note that conformer 81 was the same structure as 7 but was not fully converged under the AMBER* force field). This conformer was a $^{3,4}TC_{5,6}$ conformation for the ring and the exocyclic hydroxyl groups were arrayed in such a fashion as to maximize intramolecular hydrogen bonding in a clockwise fashion about the ring (Fig. 3). The C6–C7 dihedral adopted a gg orientation with hydrogen bonding to the oxygen of the seven-membered ring. The next conformer in energy according to this level of theory was conformer 3. This conformer

Table 3. Calculated conformational distribution for the β-septanoside (**4**)[a]

Conformer #	AMBER* E_{rel}	HF/6-31G* E_{rel}	Boltzmann Contribution (%)[b]	Ring Conformation[c]	C6–C7 rotamer[c]
7	1.52	0.00	37.13	$^{3,4}TC_{5,6}$	gg
81	5.11	0.00	37.13	$^{3,4}TC_{5,6}$	gg
3	0.73	0.47	16.79	$^{6,O}TC_{4,5}$	gg
32	3.42	1.59	2.53	$^{4,5}TC_{2,3}$	gg
13	2.10	2.00	1.26	$^{6,O}TC_{4,5}$	gg
1	0.00	2.01	1.24	$^{6,O}TC_{4,5}$	gt
2	0.65	2.24	0.85	$^{6,O}TC_{4,5}$	gt
5	1.19	2.24	0.85	$^{6,O}TC_{4,5}$	gt
67	4.72	2.30	0.77	$^{3,4}TC_{5,6}$	tg
16	2.36	2.91	0.27	$^{4,5}TC_{2,3}$	gt
18	2.59	3.19	0.17	$^{5}C_{1,2}$	gg
19	2.67	3.33	0.13	$^{6,O}TC_{4,5}$	gg
72	4.84	3.37	0.12	$^{3,4}TC_{5,6}$	gg
35	3.50	3.48	0.10	$^{1,2}TC_{6,O}$	gg
12	2.08	3.74	0.07	$^{1,2}TC_{3,4}$	gt
65	4.69	3.74	0.07	$^{1,2}TC_{3,4}$	gt
10	1.84	3.79	0.06	$^{6,O}TC_{4,5}$	gt
44	4.03	3.94	0.05	$^{3,4}TC_{5,6}$	gt
40	3.94	3.95	0.05	$^{6,O}TC_{4,5}$	gg
88	5.18	4.01	0.04	$^{3}C_{6,O}$	gg
9	1.80	4.14	0.03	$^{3,4}TC_{5,6}$	gt
8	1.76	4.14	0.03	$^{3,4}TC_{5,6}$	gt
26	3.06	4.26	0.03	$^{6,O}TC_{4,5}$	gt
36	3.52	4.26	0.03	$^{6,O}TC_{4,5}$	gt
20	2.74	4.32	0.03	$^{6,O}TC_{4,5}$	gt
11	2.02	4.38	0.02	$^{5}C_{1,2}$	gt
41	3.96	4.41	0.02	$^{3,4}TC_{5,6}$	gt
45	4.04	4.41	0.02	$^{3,4}TC_{5,6}$	gt
27	3.17	4.44	0.02	$^{6,O}TC_{4,5}$	gt
38	3.70	4.44	0.02	$^{6,O}TC_{4,5}$	gt
4	1.07	4.47	0.02	$^{6,O}TC_{4,5}$	gt
33	3.43	4.60	0.02	$^{3,4}TC_{5,6}$	gt
28	3.21	4.64	0.01	$^{6,O}TC_{4,5}$	gg
56	4.25	4.80	0.01	$^{3,4}TC_{5,6}$	gg
17	2.39	5.04	0.01	$^{1,2}TC_{6,O}$	gt

[a] Relative energies for each conformer, at each level of theory, are in kcal/mol.
[b] The Boltzmann contribution, as a percentage, is determined based on the relative energies calculated at the HF/6-31G* level of theory.
[c] From HF/6-31G* optimized geometries.

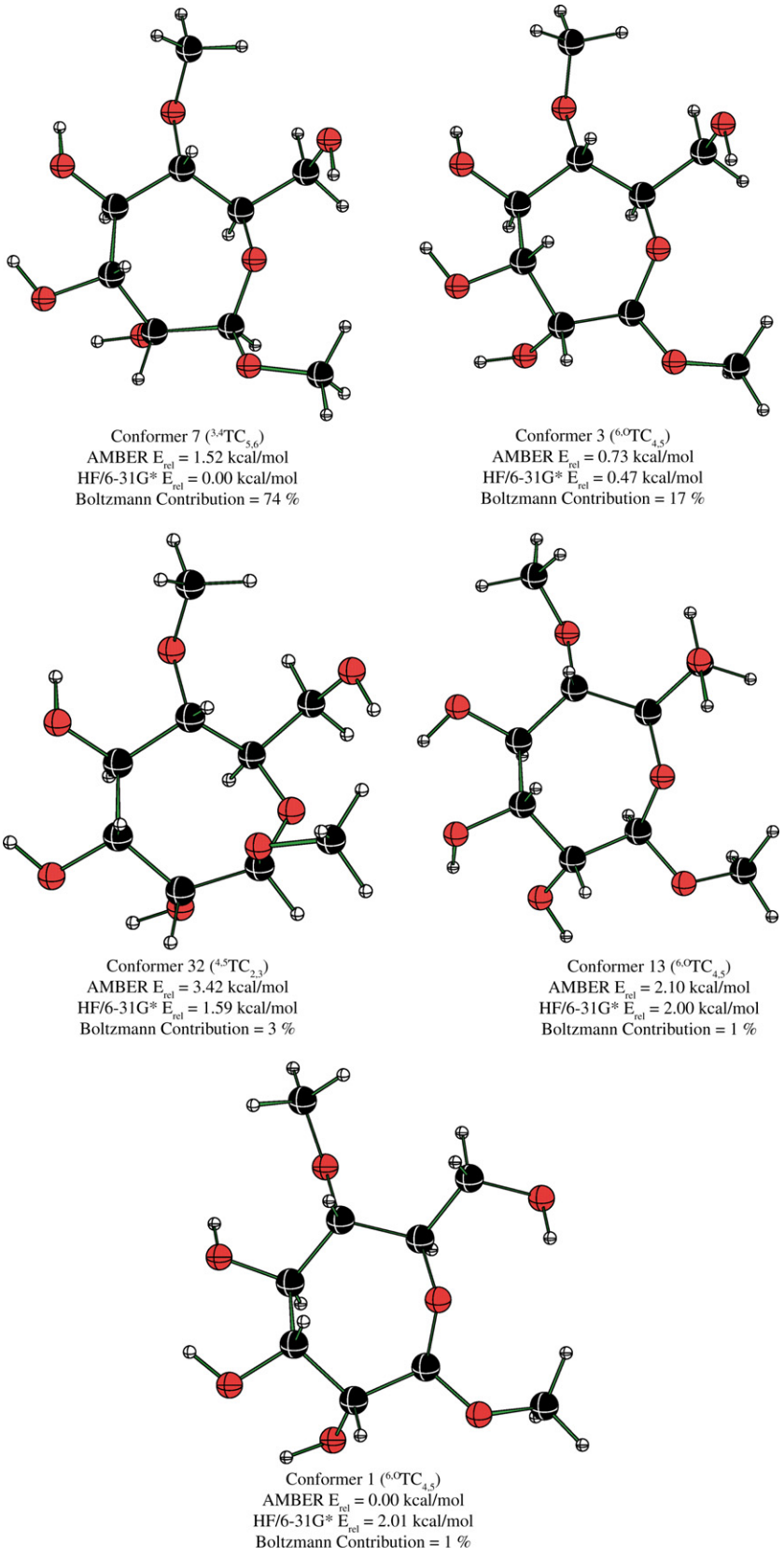

Figure 3. The lowest energy conformers of β anomer (**4**). The conformer number, ring conformation, relative energies at the AMBER and HF/6-31G* levels of theory, as well as the contribution to the Boltzmann distribution are also shown.

adopted a $^{6,O}TC_{4,5}$ conformation for the ring and intramolecular hydrogen bonding by the hydroxyl groups, this time oriented in a counter-clockwise fashion. The C6–C7 dihedral of this conformer adopted a gg orientation. The global minimum according to the AMBER* force field (conformer 1) was predicted by the HF/6-31G* level of theory to be 2 kcal/mol higher in energy than the HF/6-31G* global minimum. It adopted a $^{6,O}TC_{4,5}$ conformation with the exocyclic hydroxyl groups being hydrogen bonded in a clockwise fashion and a C6–C7 dihedral angle for the gt orientation. This was a significant difference not only in energy but also in the preferred conformation of the septanose ring. To verify that this difference in the preferred conformation was not a factor of large changes in geometry from the AMBER* to the HF/6-31G* optimization, the geometries were compared and showed very little difference in the geometry after the HF/6-31G* optimization.

The Boltzmann distributions calculated for **4** predict significantly more flexibility in the septanose ring. This is dramatically different from what had previously been observed not only for **3** but also for **1** and **2**. Intramolecular hydrogen bonding was, however, very strongly preferred, although it was possible for the hydrogen bonding to occur in different arrays (clockwise or counter-clockwise) about the molecule. There was also some flexibility about the C6–C7 dihedral angle. This exocyclic group could be oriented in a gg or gt orientation. It is of note that the Boltzmann distribution as calculated at this level of theory predicts that the molecule will rarely sample the C6–C7 tg orientation as such conformers contribute less than 1% to the total Boltzmann distribution.

2.7. Gas-phase and PCM B3LYP/6-311+G** single-point energy calculations for 4

Single-point energy calculations at the B3LYP/6-311+G** level of theory significantly altered the relative energetics of these lowest energy conformations and thus changed the relative contributions of each conformer to the Boltzmann distribution (Table 4). Gas-phase B3LYP/6-311+G** single-point energy calculations predicted that the global minimum would be conformer 3 and that this conformer would contribute approximately 36% to the Boltzmann distribution. This was noticeably different from the HF/6-31G* results where this conformer contributed only 15% to the distribution. The gas-phase B3LYP results predicted nearly equal contributions between the $^{3,4}TC_{5,6}$ and $^{6,O}TC_{4,5}$ conformations of the septanose ring rather than the overwhelming preference for the $^{3,4}TC_{5,6}$ conformer according to HF theory. The results using PCM to model the effect of the dielectric of methanol at the B3LYP/6-311+G** level of theory gave even more significantly different results where conformer 13 is predicted to be the global minimum. This conformation was a $^{6,O}TC_{4,5}$ conformer. The relative contribution to the Boltzmann distribution of this conformer was, however, only 15%. The solvation model appeared to predict a more diverse sampling of the conformational space available to β-anomer **4** with no one conformer dominating this distribution.

2.8. Calculated NMR coupling constants for 3 and 4

NMR coupling constants were calculated for all conformations within 5 kcal/mol of the global minimum according to the HF/6-31G* level of theory. These conformers were likewise demonstrated to be within at least 4 kcal/mol of the global minimum when single-point energy calculations were performed at the B3LYP/6-311+G** and PCM B3LYP/6-311+G** levels of theory. The calculations for the coupling constants were made at the PW91PW91/IGLO-III level of theory as implemented in the Gaussian 03 software package. We have confirmed that the Gaussian 03 software package, when used for the calculation of $^3J_{H,H}$ coupling constants provides results comparable to those calculated using the deMon software package as we have done in prior studies by this group[7] (see Supplementary data for details). We have also confirmed that the computed gas-phase NMR coupling constants are similar to the coupling constants calculated when using the PCM method to model the effect of the dielectric constant of the solvent (see Supplementary data). The calculated coupling constants for each individual conformer were then multiplied by the respective contribution to the Boltzmann distribution for each conformer to arrive at appropriate weighted values for each coupling constant. The resultant weighted values were then summed to determine the predicted overall coupling constants for the molecule. The calculated coupling constants as well as a comparison to experimentally determined coupling constants are provided in Tables 5 and 6.

The data in Table 5 clearly demonstrate that there is an excellent agreement between the calculated NMR coupling constants and the experimentally determined values for α-anomer **3**. All calculations are within 1 Hz of the experimental values for the coupling constants, which are diagnostic of the ring conformation. The major difference between the experimental and calculated coupling constants is observed in the coupling constants associated with conformation about the C6–C7 bond. These values differ by more than 1 Hz when comparing experiment with calculation. This may be due to the computational methods over-estimating the importance of hydrogen-bonding interactions between the C7 hydroxyl group and the ring oxygen. It is also possible that experimentally, coordination of **3** with a solvent molecule may significantly alter the C6–C7 conformational preference, an aspect neglected in our calculations.

Table 4. Calculated conformational distribution for the β-septanoside anomer (**4**)[a] as calculated at different levels of theory

Conformer #	AMBER* E_{rel}	HF/6-31G* E_{rel}	B3LYP/6-311+G** (gas phase) E_{rel}	PCM B3LYP/ 6-311+G** E_{rel}	HF/6-31G* Boltzmann contribution (%)	B3LYP/6-311+G** Boltzmann contribution (%)	PCM B3LYP/ 6-311+G** Boltzmann contribution (%)
7	1.52	0.00	0.54	1.17	37.13	14.48	1.79
81	5.11	0.00	0.54	1.17	37.13	14.50	1.78
3	0.73	0.47	0.00	0.11	16.79	35.96	17.45
32	3.42	1.59	1.76	3.67	2.53	1.85	0.02
13	2.10	2.00	0.78	0.00	1.26	9.60	17.94
1	0.00	2.01	1.24	0.89	1.24	4.42	3.24
2	0.65	2.24	0.93	0.23	0.85	7.54	7.24
5	1.19	2.24	0.93	0.23	0.85	7.53	7.26
67	4.72	2.30	2.63	2.92	0.77	0.42	0.12
16	2.36	2.91	2.92	3.01	0.27	0.26	0.09
18	2.59	3.19	3.35	4.13	0.17	0.13	0.02
19	2.67	3.33	3.27	3.12	0.13	0.14	0.10
72	4.84	3.37	3.67	1.49	0.12	0.07	1.17
35	3.50	3.48	2.98	3.48	0.10	0.23	0.05
12	2.08	3.74	3.99	3.56	0.07	0.04	0.03
65	4.69	3.74	3.99	3.56	0.07	0.04	0.03
10	1.84	3.79	3.27	3.56	0.06	0.14	0.03
44	4.03	3.94	3.95	2.20	0.05	0.05	0.58
40	3.94	3.95	3.05	0.68	0.05	0.21	4.86
88	5.18	4.01	4.04	5.96	0.04	0.04	0.00
9	1.80	4.14	3.67	4.56	0.03	0.07	0.01
8	1.76	4.14	3.67	4.56	0.03	0.07	0.01
26	3.06	4.26	2.67	0.50	0.03	0.40	7.51
36	3.52	4.26	2.67	0.50	0.03	0.40	7.47
20	2.74	4.32	3.44	0.89	0.03	0.11	2.60
11	2.02	4.38	4.13	4.06	0.02	0.03	0.02
41	3.96	4.41	4.21	2.59	0.02	0.03	0.37
45	4.04	4.41	4.21	2.59	0.02	0.03	0.37
27	3.17	4.44	2.82	0.26	0.02	0.31	8.71
38	3.70	4.44	2.82	0.26	0.02	0.31	8.67
4	1.07	4.47	2.82	2.94	0.02	0.31	0.06
33	3.43	4.60	4.12	2.50	0.02	0.03	0.29
28	3.21	4.64	3.08	2.85	0.01	0.20	0.11
56	4.25	4.80	4.44	4.37	0.01	0.02	0.01
17	2.39	5.04	4.16	4.69	0.01	0.03	0.01

[a] Relative energies for each conformer, at each level of theory, are in kcal/mol.

The comparison between experiment and computation provides confidence in assigning the conformation of the septanose ring of **3**. It is apparent that the ring adopts a $^{3,4}TC_{5,6}$ conformation.

For β-anomer **4**, however, as shown in Table 6, the data are much more difficult to decipher. It appears that the gas-phase HF and B3LYP computational methods, and their corresponding energy-weighted Boltzmann factors, were not successful in reproducing the experimental coupling constants for this molecule. The calculations predict that β-anomer **4** will be much more flexible than α-anomer **3**. There are many different conformations of the septanose ring that are energetically accessible for **4**. As such, it is vital for the computational methods to be extremely accurate at predicting these slight differences in the energetics of the different conformers. As such, using the weighting as determined at the HF/6-31G* level of theory results in a very poor prediction of the experimental coupling constants. Likewise, the gas-phase B3LYP/6-311+G** single-point energy calculations were unable to correct the Boltzmann distribution sufficiently to reproduce all of the experimental results. Consideration of an implicit solvation treatment with the polarizable continuum model in the single-point energy calculations, however, does appear to give good correlation with the experimental values for methanol. Of course, our computational study does not include explicit solvation of the septanoside, and these solute–solvent interactions will also be important for a complete description of the solute's properties, such as the C6–C7 bond as discussed below. It appears that the effect of solvent is important in determining the conformation that the septanose ring is likely to adopt. This is not surprising because there are so many conformations of similar energy available to the molecule. Using the PCM B3LYP/6-311+G** data, we

Table 5. Calculated and experimental $^{3}J_{H,H}$ and $^{1}J_{C,H}$ coupling constants (Hz) for α-anomer **3**

Coupling constant	HF[a]	B3LYP[b]	PCM B3LYP[c]	Experiment[d,e]	Sim.[g]
$^{3}J_{1,2}$	5.22	5.22	5.40	6.2	5.95
$^{3}J_{2,3}$	8.49	8.49	8.59	8.5	8.78
$^{3}J_{3,4}$	7.74	7.74	7.57	7.7	7.82
$^{3}J_{4,5}$	7.37	7.36	7.10	7.4	7.40
$^{3}J_{5,6}$	8.75	8.73	8.79	10.3	10.12
$^{3}J_{6,7R}$	1.39	1.73	3.10	4.4	4.30
$^{3}J_{6,7S}$	2.51	2.54	2.32	2.4	2.60
$^{2}J_{7R,7S}$	9.75	9.72	9.22	11.7	11.40
$^{1}J_{C,H}$	145.99	145.97	145.14	163.6[f]	

[a] Values calculated at the PW91PW91/IGLO-III level using the HF/6-31G* geometries with Gaussian 03 and the HF/6-31G* Boltzmann weightings from the conformational distribution.
[b] Values calculated at the PW91PW91/IGLO-III level using the HF/6-31G* geometries with Gaussian 03 and the B3LYP/6-311+G** Boltzmann weightings from the conformational distribution.
[c] Values calculated at the PW91PW91/IGLO-III level using the HF/6-31G* geometries with Gaussian 03 and the PCM B3LYP/6-311+G** Boltzmann weightings from the conformational distribution.
[d] Observed coupling constants from 700 MHz ^{1}H NMR experiments.
[e] Coupling constant error ±0.22 Hz for $^{3}J_{H,H}$ and ±4.9 Hz for $^{1}J_{C,H}$ determination.
[f] The $^{1}J_{C,H}$ value measured by ^{1}H coupled ^{13}C NMR was 166.4 ± 0.28 Hz.
[g] Values used for simulation by NMRSim.

Table 6. Calculated and experimental $^{3}J_{H,H}$ and $^{1}J_{C,H}$ coupling constants (Hz) for β-anomer **4**

Coupling constant	HF[a]	B3LYP[b]	PCM B3LYP[c]	Experiment[d,e]	Sim.[g]
$^{3}J_{1,2}$	1.00	3.28	5.03	5.8	5.90
$^{3}J_{2,3}$	2.08	3.59	4.96	2.7	3.00
$^{3}J_{3,4}$	8.13	8.36	8.66	8.3	8.34
$^{3}J_{4,5}$	7.69	7.64	7.35	5.8	5.73
$^{3}J_{5,6}$	8.48	8.47	8.50	9.7	9.63
$^{3}J_{6,7R}$	1.28	2.62	4.81	—	6.40[h]
$^{3}J_{6,7S}$	2.50	2.56	2.22	2.0	1.99
$^{2}J_{7R,7S}$	9.80	9.76	9.09	11.4	11.40
$^{1}J_{C,H}$	140.46	137.99	135.69	163.0[f]	

[a] Values calculated at the PW91PW91/IGLO-III level using the HF/6-31G* geometries with Gaussian 03 and the HF/6-31G* Boltzmann weightings from the conformational distribution.
[b] Values calculated at the PW91PW91/IGLO-III level using the HF/6-31G* geometries with Gaussian 03 and the B3LYP/6-311+G** Boltzmann weightings from the conformational distribution.
[c] Values calculated at the PW91PW91/IGLO-III level using the HF/6-31G* geometries with Gaussian 03 and the PCM B3LYP/6-311+G** Boltzmann weightings from the conformational distribution.
[d] Observed coupling constants from 700 MHz ^{1}H NMR experiments.
[e] Coupling constant error ±0.22 Hz for $^{3}J_{H,H}$ and 4.9 Hz for $^{1}J_{C,H}$ determination.
[f] The $^{1}J_{C,H}$ value measured by ^{1}H coupled ^{13}C NMR was 157.5 ± 0.28 Hz.
[g] Values used for simulation by NMRSim.
[h] Estimated value used in the simulation of ^{1}H NMR.

are able to reproduce the experimental values with fairly good accuracy. It should be noted, however, that the $^{3}J_{2,3}$ coupling constant remains approximately 2.4 Hz larger than that observed experimentally. Likewise, there is a smaller deviation in the $^{3}J_{4,5}$ coupling constant (a difference of 1.5 Hz). Because of these noticeable differences, we have less confidence in assigning the absolute conformation being adopted by the septanose ring. The calculated data indicate that the septanose ring will adopt both the $^{6,O}TC_{4,5}$ (93.2% of the Boltzmann distribution) and $^{3,4}TC_{5,6}$ (6.6%) conformations. These values seem to be reasonably consistent with the experimental values as manifested by the $^{3}J_{H,H}$ coupling constants. We therefore tentatively assign this as the conformational distribution for the septanose ring of **4**.

2.9. Determination of configuration

The assignment of the anomeric configuration of septanosides **3** (α) and **4** (β) was based on the information gathered in their preparation and from the collected NMR data. The rationale draws significantly from our earlier analysis of methyl septanosides **1** and **2**.[7]

The chromatographic behavior of compounds **11** and **12**, prepared by the epoxidation of oxepine **6** followed by methanolysis of the intermediate 1,2-anhydroseptanose, was reminiscent of the products of epoxidation/methanolysis of the original oxepine **7**. That is, the higher R_f material was assigned as the α anomer in the original system and the lower R_f material was assigned as the β with a product ratio of 1:3 α:β. By analogy, we have assigned the higher R_f material that resulted from the epoxidation and methanolysis of **6** as structure **11** and the lower R_f material as **12**. The ratio of 1:2 (α:β) for **11**:**12** is nearly the same as the parent system.

NMR spectra provided an additional insight into the identity of **3** and **4**. First, the general appearance of the ^{1}H NMR spectrum of **3** was very similar to **1**, especially the low chemical shift dispersion of the H2, H3, and H4 resonances in each (a comparison of the ^{1}H NMR spectra of **1** and **3** is in the Supplementary data). We have also used ^{13}C chemical shifts as diagnostics for anomeric configuration of septanosides in previous systems. In the limited examples we have collected,[7,14,17,18] the trend is that δ C1 of β-septanosides is slightly downfield relative to α-septanosides. The ^{13}C NMR measured values for δ C1 of **3** is 106.1 ppm and that of **4** is 109.3 ppm. These data support the configurations we have assigned and are consistent with the earlier methyl septanoside assignments. For comparison, a list of C1 ^{13}C NMR chemical shifts for selected methyl septanosides is provided in the Supplementary data. Additionally, their qualitative relationship (α-upfield, β-downfield) is supported by calculated chemical shift values. For example, the calculated ^{13}C δ (ppm) for **3** at various levels of theory are 118.71 (HF/6-31G*), 118.70 (B3LYP/6-311+G**), and 118.22 (PCM B3LYP/6-311+G**) and 119.71, 122.09, 121.98 for **4** at the same levels. Next, the H1 signal of α-anomer

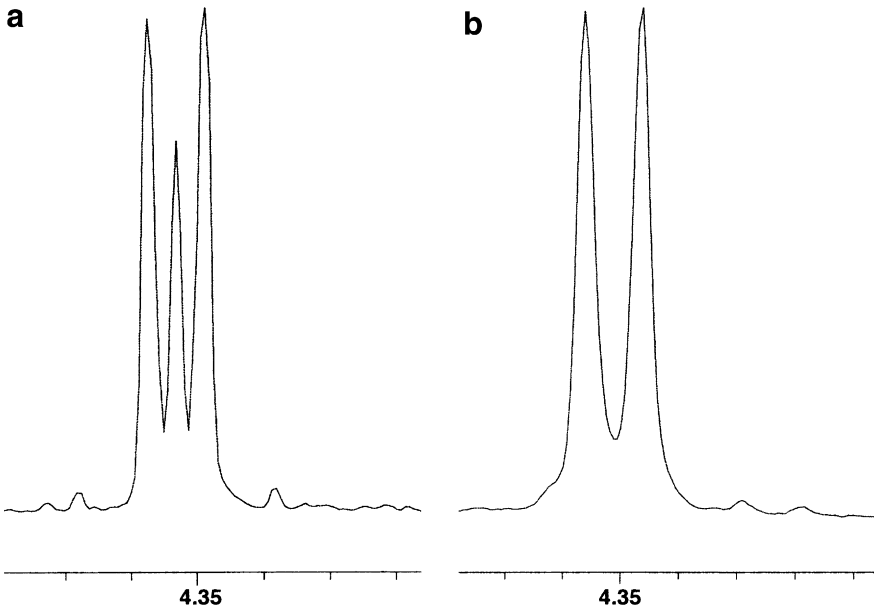

Figure 4. Detail of ^{1}H NMR spectra showing H1 of (a) α-anomer **3** and (b) β-anomer **4**.

3 was unique in displaying an additional coupling that was not observed for β-anomer **4** as shown in Figure 4. Because H2 and H3 of **3** have almost identical chemical shifts, the H1, H2, and H3 protons make an ABX spin system[19] that shows complex splitting even at 700 MHz. Further, the large $^{3}J_{H,H}$ coupling constant for H2–H3 in **3** is likely responsible for the complex splitting observed at H1. This phenomenon is not observed for **4** due to the lower magnitude of the H2–H3 coupling. As will be presented below, diagnostic $^{3}J_{H,H}$ couplings were also used in the determination of the ring conformation of **3** and **4**. The agreement that was reached between the predicted $^{3}J_{H,H}$ values, calculated from their low energy conformations, and the $^{3}J_{H,H}$ observed in ^{1}H NMR spectroscopy support the assignment of the α- and β-stereochemistry of **3** and **4**, respectively.

2.10. Ring conformations

The comparison of the NMR observed $^{3}J_{H,H}$ coupling constants to the calculated values determines the low energy ring conformations in our system. The values of $^{3}J_{H,H}$ for α-anomer **3** and β-anomer **4** from calculation, ^{1}H NMR spectra, and simulation are listed in Tables 5 and 6. Each table gives calculated $^{3}J_{H,H}$ values from Boltzmann weightings computed at three levels of theory: HF-6-31G*, B3LYP/6-311+G**, and PCM B3LYP/6-311+G**. Observed $^{3}J_{H,H}$ values were measured from ^{1}H NMR spectra of **3** and **4** dissolved in CD_3OD and collected at 25°C and 700 MHz. Individual ^{1}H NMR resonances for H1–H7 of **3** and **4** were assigned by one-dimensional ^{1}H and H,H COSY experiments. The ^{1}H NMR spectra of both **3** and **4** showed significant chemical shift overlap; however, the spectra collected at 700 MHz were sufficient for the determination of the ring conformations. Due to overlap of the C6 and C7R protons of **4**, experimentally determined rotamer populations of the exocyclic C6–C7 bond were not obtained experimentally. For the couplings reported, errors in the $^{3}J_{H,H}$ values were both ±0.22 Hz as governed by the digital resolution of the free induction decays of **3** and **4**. NMRSim[36] was used to simulate the one-dimensional ^{1}H NMR spectra and were compared to the experimental spectra by visual inspection. The simulation of the spectra for **3** and **4** was conducted to support the experimental values.

The data in Tables 5 and 6 provide an insight into the preferred conformations of **3** and **4**. There is a general agreement between the calculated and the experimental $^{3}J_{H,H}$ coupling constants. The calculated coupling constants are within 1–1.5 Hz of the experimental values, and a consistent trend in the discrepancies between the calculated and experimental was not observed. The agreement indicates that the calculated Boltzmann distribution of conformers is representative of the solution conformation of each septanoside.

As in the parent system (**1** and **2**), *essentially one ring conformation is populated by α-anomer* **3**. The preferred conformation for **3** was $^{3,4}TC_{5,6}$. The $^{3}J_{2,3}$ and $^{3}J_{3,4}$ values are diagnostic of both relative stereochemistry and conformation in this system. From the calculations, α-anomer **3** should have $^{3}J_{2,3}$ of 8.49 Hz and a $^{3}J_{3,4}$ of 7.74 Hz (large, large) and the β-anomer **4** should have $^{3}J_{2,3}$ of 5.05 Hz and a $^{3}J_{3,4}$ of 8.69 Hz (small, large). The experimental data reflect the pattern set by the calculated values, delivering coupling constants of 8.5 and 7.7 Hz for **3** and 2.7 and 8.3 Hz for **4**. The factors that govern the preference for the $^{3,4}TC_{5,6}$ conformation

adopted by **3** include placing the aglycon OCH_3 group in an isoclinal position to minimize steric interactions with the rest of the ring[8a,b] and also orienting the aglycon axially due to the anomeric effect.[20,21] Other substituents, including the exocyclic hydroxymethyl group (C7 unit) are oriented equatorially to minimize steric interactions.

The picture for β-anomer **4** is more complicated. The data indicate that **4** populates a group of related conformers ($^{6,O}TC_{4,5}$, $^{3,4}TC_{5,6}$, $^{5}C_{1,2}$, $^{4,5}TC_{2,3}$, $^{3}C_{6,O}$, and $^{1,2}TC_{6,O}$) rather than adopting just one ring conformation. Of these, the $^{6,O}TC_{4,5}$, $^{3,4}TC_{5,6}$, and $^{5}C_{1,2}$, conformations are all represented with varying magnitudes depending on the level of theory used (Table 4). These conformers are adjacent to each other on the pseudorotational itinerary[11] and place their substituents in an equatorial position. The $^{4,5}TC_{2,3}$ conformer of septanoside **4**, which is also populated up to 2% in the Boltzmann distribution, is farther away on the pseudorotational itinerary. The $^{4,5}TC_{2,3}$ conformation is distinct in placing the aglycon in a pseudoaxial position, presumably because of the anomeric effect. The clearest implication of the results is that the addition of the methyl group at the C5, and by extension, glycosylation at C5, does not significantly alter the preferred conformations adopted by α-septanoside **3**, but does result in some flexibility in β-septanoside ring **4**.

The agreement between the calculated and observed conformational distributions (as determined by $^{3}J_{H,H}$ coupling constant analysis) for **3** and **4** varies based on the level of theory/basis set that was used to determine the relative energies of representative conformations. For **3**, the HF-6-31G*, B3LYP/6-311+G**, and PCM B3LYP/6-311+G** calculations consistently place the $^{3,4}TC_{5,6}$ conformation as the global low energy conformation and agree well with the $^{3}J_{H,H}$ determined conformation. Overall, the agreement reinforces the notion that the α-septanoside structures, such as **1** and **3**, adopt one low energy conformation and is relatively rigid. In contrast, none of the calculated conformational distributions for **4** seems to perfectly describe the $^{3}J_{H,H}$ values observed in ^{1}H NMR. Neither do the $^{3}J_{H,H}$ values of individual conformers of **4**. The best approximation is provided using the values from the PCM B3LYP/6-311+G** treatment. Conformers representing >2% of the PCM B3LYP Boltzmann distribution include the closely related conformations $^{6,O}TC_{4,5}$, $^{5}C_{1,2}$, and $^{3,4}TC_{5,6}$. An additional conformation, $^{4,5}TC_{2,3}$, is present in the HF and B3LYP calculations at roughly 2%, but does not contribute at the PCM B3LYP level. The underlying implication of these results, which is key to the present investigation, is that a number of conformations, nearby in energy for **4**, are populated. It suggests, although does not require, that the alkylation/glycosylation at C5 of the β-septanosides may result in a more flexible, less rigid ring structure. The computational and experimental data support the idea that β-septanoside **4** is flexible. First, we argue that the agreement between the experimental $^{3}J_{H,H}$ values and those calculated using Boltzmann weightings based on the PCM-B3LYP/6-311+G** calculations agree sufficiently to describe the low energy conformations of **4**. Second, looking at the PCM energies and Boltzmann distribution of **4**, it is apparent that the two TC minima, the $^{6,O}TC_{4,5}$ and the $^{3,4}TC_{5,6}$ comprise >99% of the species at equilibrium (Table 4). These two TCs are adjacent to one another on the TC/C pseudorotational itinerary for the seven-membered rings.[11] Looking at the relative (unweighted) energies of each shows that all of the $^{6,O}TC_{4,5}$ conformers average to 1.13 kcal/mol and the $^{3,4}TC_{5,6}$ conformers average to 2.74 kcal/mol. Further, the $^{5}C_{1,2}$ is also present in the conformer distribution and its average energy is 4.10 kcal/mol; $^{5}C_{1,2}$ is also the chair conformer which can be considered the transition state between the $^{6,O}TC_{4,5}$ and $^{3,4}TC_{5,6}$ conformers.[11] The calculated energy (~4 kcal/mol) of the $^{5}C_{1,2}$ therefore approximates the barrier to interconversion between these two adjacent TCs. The barrier between the $^{6,O}TC_{4,5}$ and the $^{3,4}TC_{5,6}$ conformers is relatively low,[22] suggesting that interconversion between the two conformations occurs readily even at low temperatures. ^{1}H NMR spectra for β-septanoside **4** were collected at −40 °C in CD_3OD (500 MHz) and showed a greater chemical shift dispersion, but with very similar ^{3}J coupling constants (Supplementary data).

The picture developed in this analysis fits the description of flexibility introduced earlier; that is, multiple conformations of similar energies are available to a given structure (**4**), and it populates each of these conformers, and with a transition state structure of low energy (~4 kcal/mol) that allows interconversion between these conformations. The populations of the two TC conformers, based on theory, still shows a strong preference for the $^{6,O}TC_{4,5}$ conformation. However, it may be that the methyl group at C5 of **4** does not fully approximate the steric bulk of an additional pyranose or septanose sugar at its reducing end. We would expect that an increased steric bulk, as from another carbohydrate ring at this position, may further change the population of the two TC conformers. Synthetic efforts toward preparing such disaccharide analogs are in process to test this hypothesis. Heteronuclear ^{1}J values ($^{1}J_{C,H}$) were also explored as another diagnostic for conformation and subsequently configuration. Calculations showed that the magnitude of $^{1}J_{C,H}$ for the 5-*O*-methyl α-septanoside **3** was consistently greater than for the 5-*O*-methyl β-septanoside **4**. For example, at the PCM B3LYP level of theory, the $^{1}J_{C,H}$ for **3** was 145.45 and 135.54 Hz for **4**. The qualitative trend in these $^{1}J_{C,H}$ values is in good agreement with those calculated and observed for the parent septanosides **1** and **2**.[7] The experimental $^{1}J_{C,H}$ values collected

from ^{13}C-coupled HMQC spectra were inconclusive. For α-septanoside **3**, the measured $^{1}J_{C,H}$ was 163.6 Hz and for β-septanoside **4**, 163.0 Hz; these values are essentially the same and therefore gave little insight into the configuration/conformation of **3** and **4**. For comparison, the measured ^{1}J coupling constants for **1** and **2** were 167.9 and 160.1 Hz, respectively. The calculated values are systematically lower than the observed values; this was also true in the parent system (**1** and **2**).

2.11. Rotamer populations

The experimental coupling constants ($^{3}J_{H6,H7R}$ and $^{3}J_{H6,H7S}$) that describe the C7 exocyclic hydroxymethyl group in **3** and **4** were analyzed. The values are diagnostic for the preferred orientation of the hydroxymethyl group; a correlation of rotamer preference and ring conformation has been noted.[23] Chart 2 shows the H–C–C–H dihedral angles for the tg, gt, and gg conformers. Rotamer distributions were calculated using the appropriate $^{3}J_{H,H}$ values to solve Eqs. 1–3.

$$0.57X_{tg} + 9.70X_{gt} + 4.11X_{gg} = {}^{3}J_{H6\text{–}H7R} \quad (1)$$

$$9.79X_{tg} + 3.74X_{gt} + 0.71X_{gg} = {}^{3}J_{H6\text{–}H7S} \quad (2)$$

$$X_{tg} + X_{gt} + X_{gg} = 1 \quad (3)$$

For the solutions to Eqs. 1–3 to be physically realistic (all mole fractions X to be positive), the downfield chemical shift was H7*S* and the upfield chemical shift was H7*R*. This trend corresponds to earlier furanose and pyranose examples.[24,25] The coefficients for Eqs. 1 and 2 were those that we used in the original (parent) system. Table 7 collects the rotamer populations of compounds **3** and **4** based on the conformer populations generated by computation (calcd) and by solving Eqs. 1–3 using the experimentally observed ^{3}J values (obs).

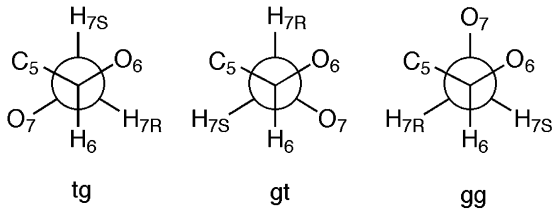

Chart 2.

Table 7. Comparison of C6–C7 rotamer populations in **3** and **4**

	3		**4**	
	Calcd[a]	Obs	Calcd[b]	Obs[c]
X_{tg}	0	14	<1	0
X_{gt}	5	14	62	41
X_{gg}	95	72	38	59

[a] Values calculated using HF/6-31G* Boltzmann distribution.
[b] Values calculated using PCM-B3LYP/6-311+G** Boltzmann distribution.
[c] Values used to calculate the populations for **4** used the simulated $^{3}J_{H,H}$ values.

A considerable preference for the gg conformation about C6–C7 in α-septanoside **3** was observed both by calculation and spectroscopy (Table 7). The gg rotamer was also observed in our earlier analysis of α-septanoside **1** and also in the solid state of a related methyl α-2-deoxy-septanoside.[26] In all of these cases, the gg rotamer is likely to be stabilized by a hyperconjugative interaction between σ(C6–H6)→σ*(C7–O7). The interactions between the C6 hydroxymethyl group and solvent[27] also influence which rotamers for **3** and **4** are accessed. Additionally, potential steric interactions between the exocyclic methyl group at C5 and the C6 hydroxymethyl group may likely disfavor the tg rotamer resulting in a low calculated and observed occupancy. The inspection of the calculated low energy conformations of both **3** and **4** showed that the C5 methyl group is eclipsing (or nearly eclipsing) the C5 hydrogen. This C5–O5 conformation, although not thoroughly explored in this work, minimizes the steric interaction while leaving the C5 oxygen lone pairs to accept hydrogen bonds that are present, for example, in conformers 6, 10, and 1 of **3**.

Due to the overlap of the H6 and H7*R* protons for β-septanoside **4**, we used the simulated $^{3}J_{H,H}$ values to determine its C6–C7 rotameric distribution. The values for $^{3}J_{H6,H7R}$ and $^{3}J_{H6,H7S}$ from the simulation are reasonable to use based on two arguments. First, the simulated $^{3}J_{H6,H7S}$ number (1.99 Hz) is essentially the same as the experimentally measured (2.0 Hz) value. Also, using 6.4 Hz for the $^{3}J_{H6,H7R}$ value was the best fit between the simulated and observed ^{1}H spectra. Second, based on the greater chemical shift dispersion at −40 °C, the experimental numbers could be used to estimate rotamer populations at this temperature. They were $X_{gg} = 69\%$, $X_{gt} = 28\%$, and $X_{tg} = 3\%$. These numbers are similar to those at 25 °C and maintain a preference for the gg rotamer, and only increasing its magnitude. The calculated rotamer distribution is close to that observed for the parent β-septanoside **2** (X_{tg} 10%, X_{gt} 60%, X_{gg} 30%). The predicted preference of the gt rotamer may again be based on the ability of the exocyclic hydroxyl groups to be involved in hydrogen bonds. The C7 hydroxy group can hydrogen bond with the C6 (ring) oxygen in this (gt) conformation. The experimental values for **4**, however, show a preference, as with **3**, for the gg conformation. There may be steric effects that disfavor the tg and gt conformations of the C6–C7 bond in **4** that are in addition to the favorable hyperconjugative effect in the gg conformation mentioned earlier.

3. Conclusions

Methyl 5-*O*-methyl-α-D-*glycero*-D-idoseptanoside (**3**) and methyl 5-*O*-methyl-β-D-*glycero*-D-guloseptanoside

(**4**) were synthesized as models of the reducing-end residue of septanose disaccharides. The methyl group at C5 of **3** and **4** served as a surrogate at the non-reducing end sugar of the disaccharide; its use simplified the synthetic, computational and spectroscopic efforts. The methyl septanosides were synthesized from carbohydrate-based oxepine **6** via an oxidative glycosylation using sodium methoxide as a nucleophile. The anomeric configuration of **3** and **4** was assigned based on comparison to the previous system (**1** and **2**) and to the calculations in the conformational analysis conducted here.

Low-energy conformations of **3** and **4** were determined through a Monte Carlo search followed by molecular mechanics minimizations and geometry optimization at several levels of theory. The most significant outcome of the conformational analysis is that α-anomer **3** occupied primarily *one* ring conformation and β-anomer **4** occupied at least three ring conformations. The preferred conformations were the $^{3,4}TC_{5,6}$ conformation for **3** and the $^{6,O}TC_{4,5}$, and $^{3,4}TC_{5,6}$ for **4**.

The low-energy conformations of **3** and **4** identified by calculation were also observed by ^1H NMR spectroscopic analysis. The agreement between the calculated, observed, and simulated $^3J_{H,H}$ values was sufficient to define the low-energy conformations and assign the configuration of **3** and **4**. $^3J_{H,H}$ couplings around the C6–C7 bond were used to assign the rotamer distribution of the exocyclic hydroxymethyl group in **3** and **4**. The preferred gg conformation is the same as was observed for other methyl α-septanosides.

The combined computational and spectroscopic treatment of the methyl 5-*O*-methyl α-septanoside (**3**) presented here suggests that it adopts a relatively rigid low energy conformation that mirrors the preferences of its parent septanoside **1**. This suggests that either the methyl group at C5 did not have sufficient steric bulk to approximate glycosylation or that the conformation of the non-reducing sugar in septanose di- and oligosaccharides of this configuration will not be affected by glycosylation. Other studies have effectively utilized the methyl group as a replacement for the non-reducing end sugar, so the former argument seems unlikely.[12] Because the C5 hydroxy group is equatorial in the $^{3,4}TC_{5,6}$ conformation for both **1** and **3**, it is probable that the steric bulk added by methylation, or glycosylation, should not significantly change its preferred low energy conformation. On the other hand, methylation on the C5 hydroxyl does show some effects on the distribution of low energy conformers of β-septanoside **4**. Specifically, in addition to the $^{6,O}TC_{4,5}$ conformation that is adopted by both **2** and **4**, methyl β-5-*O*-methyl septanoside (**4**) also populates the nearby $^{3,4}TC_{5,6}$ conformation. The calculations further suggest that other conformations of **4** ($^5C_{1,2}$ and $^{4,5}TC_{2,3}$, for example) are energetically accessible and can be represented up to 2% of the Boltzmann distribution of **4** based on the level of theory used. The $^5C_{1,2}$ conformer is especially critical because it represents the transition state between the two populated low energy conformations. Together, the $^{6,O}TC_{4,5}$, $^{3,4}TC_{5,6}$, and $^5C_{1,2}$ conformations provide a reference for the barrier to interconversion between related TC conformers for septanoses and illustrate the flexibility in this system. We intend on evaluating the significance of the results collected in this investigation, particularly the flexibility of β-septanoside **4**, in our continued development of septanose carbohydrates as reagents in glycobiological applications.

4. Experimental

4.1. General methods

Unless stated otherwise, all reactions were conducted at room temperature (rt) under nitrogen atmosphere. DMDO was generated as described.[28] The reactions were monitored by TLC (silica gel, 60 Å, F_{254}, 250 μm). Visualization was conducted either under UV light or by charring with 2.5% *p*-anisaldehyde in H_2SO_4, acetic acid, and ethanol solution. Preparative chromatography was conducted on silica gel (60 Å, 32–63 μm). Melting points are uncorrected. Optical rotations were measured at 22 ± 2 °C. ^1H NMR spectra were collected at 300, 400 or 600, 700 MHz with chemical shifts referenced to $(CH_3)_4Si$ (δ_H 0.00 ppm), the residual signal in $CHCl_3$ (δ_H 7.27 ppm), or CHD_2OD (δ_H 3.31 ppm). ^{13}C NMR were collected at 75, 100 MHz and referenced to the residual signal in $CDCl_3$ (δ_C 77.2 ppm), or CD_3OD (δ_C 49.0 ppm).

4.2. 3,4,7-Tri-*O*-benzyl-5-*O*-methyl-1,2-dideoxy-D-glucohept-1-enitol (9)

Into a flame-dried round-bottom flask was added methyl triphenylphosphonium bromide (2.43 g, 6.8 mmol) and dry THF (30 mL) to make a white suspension, which was cooled to 0 °C on an ice bath. *n*-Butyllithium (6.8 mL, 1.0 M) was added dropwise with stirring and gave a clear, dark-orange solution of methylene triphenylphosphane. This solution was stirred at 0 °C for 10 min, then allowed to warm to rt over 30 min. In a separate flask, residual water was removed from 2,3,6-tri-*O*-benzyl-4-*O*-methyl-α/β-D-glucopyranose **8** (0.785 g, 1.7 mmol) via azeotropic distillation from toluene (3 × 10 mL) under reduced pressure. The residue was dissolved in dry THF (5 mL) and cooled to 0 °C on an ice bath. *n*-Butyllithium (1.7 mL, 1.0 M) was added dropwise with stirring. This solution was then added to the methylene triphenylphosphane solution via cannula and stirred for 24 h. The reaction was quenched by the addition of aq NH_4Cl and the solvent was removed under reduced pressure. The resulting

orange oil was dissolved in DCM (25 mL) and washed with brine (25 mL) and water (25 mL). The organic layer was dried (Na_2SO_4) and the solvent removed under reduced pressure. The residue was purified by column chromatography (7:3 hexane/EtOAc) to give **9** (0.5 g, 64%) as a light yellow oil: $[\alpha]_D$ +9.1 (*c* 0.8, $CHCl_3$); ^1H NMR (300 MHz, $CDCl_3$): δ 7.43–7.32 (m, 15H), 5.99–5.87 (m, 1H), 5.45 (s, 1H), 5.42–5.40 (m, 1H), 4.96 (d, $J = 11.1$ Hz, 1H), 4.74 (d, $J = 9.7$ Hz, 1H), 4.70 (d, $J = 10.0$ Hz, 1H), 4.58 (s, 2H), 4.50 (d, $J = 11.7$ Hz, 1H), 4.27 (dd, $J = 7.4$, 7.4 Hz, 1H), 4.10–4.00 (m, 1H), 3.86 (dd, $J = 7.2$, 2.6 Hz, 1H), 3.69–3.64 (m, 2H), 3.50 (dd, $J = 6.6$, 2.7 Hz, 1H), 3.43 (s, 3H); ^{13}C NMR (100 MHz, $CDCl_3$): δ 138.5, 138.4, 138.1, 135.5, 128.6, 128.5 (2), 128.4, 128.3 (2), 128.2, 128.0 (2), 127.9 (2), 127.8 (2), 127.7, 127.6, 119.3, 82.4, 81.2, 80.1, 75.0, 73.4, 71.3, 70.8, 70.0, 59.3; ESI-MS *m*/*z* $[M+Na]^+$ calcd 485.2298, found 485.2290.

4.3. 3,4,7-Tri-*O*-benzyl-5-*O*-methyl-1,2-dideoxy-6-*O*-vinyl-D-glucohept-1-ene (10)

Ethylvinyl ether (40 mL) and dry DCM (5 mL) were combined in a flame-dried round-bottom flask. To this mixture was added 1,10-phenanthroline (0.034 g, 0.186 mmol) followed by $Pd(OAc)_2$ (0.042 g, 0.186 mmol), which was allowed to stir for 15 min. To this mixture was added **9** (0.430 g, 0.93 mmol) in DCM (5 mL). The flask was fitted with a condenser and heated at reflux for 3 days. The solvent was removed under reduced pressure and the dark oily residue was purified by column chromatography (3:1 hexane/EtOAc) to give **10** (0.363 g, 80%) as a light yellow oil: $[\alpha]_D$ +3.7 (*c* 0.7, $CHCl_3$); ^1H NMR (400 MHz, $CDCl_3$): δ 7.39–7.27 (m, 15H), 6.25 (dd, $J = 13.9$, 6.5 Hz, 1H), 5.93 (ddd, $J = 17.2$, 10.4, 7.8 Hz, 1H), 5.40 (d, $J = 10.7$ Hz, 1H), 5.37 (d, $J = 17.9$ Hz, 1H), 4.90 (d, $J = 11.0$ Hz, 1H), 4.66 (d, $J = 11.5$ Hz, 1H), 4.64 (d, $J = 10.5$ Hz, 1H), 4.56 (s, 2H), 4.45 (d, $J = 11.5$ Hz, 1H), 4.36 (dd, $J = 14.1$, 1.5 Hz, 1H), 4.19 (dd, $J = 7.5$, 7.5 Hz, 1H), 4.13–4.10 (m, 1H), 4.04 (dd, $J = 6.5$, 1.5 Hz, 1H), 3.87 (dd, $J = 10.9$, 2.8 Hz, 1H), 3.74 (dd, $J = 6.8$, 3.1 Hz, 1H), 3.71 (dd, $J = 6.5$, 3.1 Hz, 1H), 3.66 (dd, $J = 10.9$, 4.9 Hz, 1H), 3.47 (s, 3H); ^{13}C NMR (100 MHz, $CDCl_3$): δ 151.1, 138.7, 138.4, 138.2, 135.4, 128.4, 128.3 (3), 128.2, 127.9, 127.7, 127.6, 127.5 (2), 119.5, 89.2, 82.2, 81.1, 79.6, 78.7, 75.2, 73.4, 70.7, 68.6, 60.4; ESI-MS *m*/*z* $[M+Na]^+$ calcd 511.2455, found 511.2451.

4.4. 1,6-Anhydro-3,4,7-tri-*O*-benzyl-5-*O*-methyl-D-glucohept-1-enitol (6)

The following reaction was conducted in a glove box. Diene **10** (0.2 g, 0.41 mmol) was dissolved in toluene (81 mL). To this solution was added 2,6-diisopropylphenylimidoneophylidenemolybdenum(VI) bis-(hexafluoro-*t*-butoxide) (Schrock catalyst) (0.078 g, 0.102 mmol) in toluene (5 mL). The mixture was stirred in the glove box for 4 h, then removed from the box and the solvent was removed under reduced pressure to give a brown oily residue. Purification by column chromatography (3:1 hexane/EtOAc) gave **6** (0.167 g, 89%) as a light brown oil: $[\alpha]_D$ +56.9 (*c* 0.7, $CHCl_3$); ^1H NMR (400 MHz, $CDCl_3$): δ 7.41–7.29 (m, 15H), 6.50 (d, $J = 7.0$ Hz, 1H), 4.77 (dd, $J = 6.9$, 6.7 Hz, 1H), 4.70–4.57 (m, 7H), 4.06 (dd, $J = 6.5$, 5.5 Hz, 1H), 3.86 (dd, $J = 5.0$, 3.9 Hz, 1H), 3.79–3.77 (m, 2H), 3.59 (dd, $J = 9.6$, 3.5 Hz, 1H), 3.40 (s, 3H); ^{13}C NMR (100 MHz, $CDCl_3$): δ 149.3, 138.4, 138.3, 138.2, 128.4 (2), 128.3, 127.9, 127.7 (2), 127.6, 127.5, 103.3, 82.1, 82.0, 81.0, 73.5, 73.1, 72.4, 70.6, 70.3, 59.1; ESI-MS *m*/*z* $[M+Na]^+$ calcd 483.2142, found 483.2148.

4.5. Methyl 3,4,7-tri-*O*-benzyl-5-*O*-methyl-α-D-*glycero*-D-idoseptanoside (11) and methyl 3,4,7-tri-*O*-benzyl-5-*O*-methyl-β-D-*glycero*-D-guloseptanoside (12)

DMDO epoxidation of **6** (0.119 g, 0.259 mmol) in DCM (2 mL) at 0 °C over 30 min was followed by solvent removal under reduced pressure. To the resulting 1,2-anhydroseptanose was added $NaOCH_3$ (0.010 g) in CH_3OH (5 mL), and the mixture was stirred overnight (12 h). The reaction mixture was quenched with water (3 mL), and the solvent was removed under reduced pressure. The residue was dissolved in DCM (20 mL), washed with water (2 × 10 mL), and dried (Na_2SO_4), and the solvent was removed under reduced pressure. The residue was purified by column chromatography (3:1 hexane/EtOAc) to give two products.

4.5.1. Methyl 3,4,7-tri-*O*-benzyl-5-*O*-methyl-α-D-*glycero*-D-idoseptanoside (11). The first fraction gave **11** (0.025 g, 19%) as a light brown oil: $R_f = 0.3$ (3:1 hexanes–EtOAc); $[\alpha]_D$ +17.3 (*c* 0.4, $CHCl_3$); ^1H NMR (400 MHz, $CDCl_3$): δ 7.38–7.29 (m, 15H), 5.02 (d, $J = 10.9$ Hz, 1H), 4.97 (d, $J = 10.9$ Hz, 1H), 4.86 (d, $J = 10.8$ Hz, 1H), 4.67 (d, $J = 12.3$ Hz, 1H), 4.63 (d, $J = 10.8$ Hz, 1H), 4.62 (d, $J = 12.3$ Hz, 1H), 4.51 (d, $J = 6.0$ Hz, 1H), 3.78–3.72 (m, 2H), 3.64–3.51 (m, 5H), 3.54 (s, 3H), 3.48 (s, 3H); ^{13}C NMR (75 MHz, $CDCl_3$): δ 138.6, 138.0, 137.6, 128.7, 128.4, 128.3, 128.1, 128.0, 127.8, 127.7, 127.6 (2), 104.1, 88.6, 81.6, 79.4, 76.3, 76.0, 73.4, 72.6, 70.3, 69.5, 60.9, 55.9; ESI-MS *m*/*z* $[M+Na]^+$ calcd 531.2353, found 531.2351.

4.5.2. Methyl 3,4,7-tri-*O*-benzyl-5-*O*-methyl-β-D-*glycero*-D-guloseptanoside (12). The second fraction gave **12** (0.044 g, 34%) as a light brown oil: $R_f = 0.2$ (3:1 hexanes–EtOAc); $[\alpha]_D$ +23.2 (*c* 0.6, $CHCl_3$); ^1H NMR (400 MHz, $CDCl_3$): δ 7.35–7.28 (m, 15H), 4.72 (d, $J = 11.5$ Hz, 1H), 4.65–4.55 (m, 5H), 4.48 (d, $J = 7.7$ Hz, 1H), 4.02–4.00 (m, 1H), 3.98–3.93 (m, 2H), 3.87–3.85

(m, 1H), 3.72–3.61 (m, 2H), 3.55 (s, 3H), 3.53–3.45 (m, 1H), 3.27 (s, 3H); ^{13}C NMR (100 MHz, $CDCl_3$): δ 138.4, 138.1, 137.9, 128.4 (2), 128.3, 128.0 (2), 127.8, 127.7, 127.6, 127.5, 106.6, 83.0, 79.0, 77.2, 77.1, 73.6, 73.4, 72.6, 72.4, 71.9, 58.2, 56.4; ESI-MS m/z $[M+Na]^+$ calcd 531.2353, found 531.2359.

4.6. Methyl 5-*O*-methyl-α-D-*glycero*-D-idoseptanoside (3)

Pd/C (10%, 0.006 g) was added to a solution of **11** (0.022 g, 0.043 mmol) in CH_3OH (10 mL). The reaction was placed under an H_2 atmosphere via a balloon, and the mixture was stirred for 4 h at rt. The balloon was removed from the flask, and the mixture was filtered through a short pad of Celite. The Celite was washed additional CH_3OH (3×5 mL). The solvent was removed from the combined filtrates by rotary evaporation under reduced pressure to give a white solid (0.010 g, 97%): $[\alpha]_D$ +101.4 (c 0.4, CH_3OH); ^{1}H NMR (700 MHz, CD_3OD): δ 4.35 (dd, $J = 6.1$, 3.1 Hz, 1H), 3.73 (dd, $J = 11.5$, 2.7 Hz, 1H), 3.65 (dd, $J = 11.7$, 4.4 Hz, 1H), 3.56 (s, 3H), 3.54 (ddd, $J = 10.4$, 4.2, 2.6 Hz, 1H), 3.46 (s, 3H), 3.41–3.35 (m, 3H), 3.17 (dd, $J = 10.4$, 7.8 Hz, 1H); ^{13}C NMR (100 MHz, CD_3OD): δ 106.1, 83.0, 81.2, 74.3, 72.0, 71.7, 63.6, 61.0, 56.3; ESI-MS m/z $[M+Na]^+$ calcd 261.0945, found 261.0962.

4.7. Methyl 5-*O*-methyl-β-D-*glycero*-D-guloseptanoside (4)

Pd/C (10%, 0.008 g) was added to a solution of **12** (0.040 g, 0.079 mmol) in CH_3OH (10 mL). The reaction was placed under an H_2 atmosphere via a balloon, and the mixture was stirred for 4 h at rt. The balloon was removed from the flask, and the mixture was filtered through a short pad of Celite. The Celite was washed additional CH_3OH (3×5 mL). The solvent was removed from the combined filtrates by rotary evaporation under reduced pressure to give a white solid (0.018 g, 96%): $[\alpha]_D$ +15.4 (c 1.0, CH_3OH); ^{1}H NMR (700 MHz, CD_3OD): δ 4.39 (d, $J = 5.9$ Hz, 1H), 3.94 (dd, $J = 8.4$, 5.7 Hz, 1H), 3.84 (dd, $J = 8.3$, 3.0 Hz, 1H), 3.82–3.80 (m, 2H), 3.63–3.55 (m, 2H), 3.49 (s, 6H), 3.13 (dd, $J = 9.6$, 5.7 Hz, 1H); ^{13}C NMR (100 MHz, CD_3OD): δ 109.3, 85.5, 80.1, 74.9, 73.4, 73.1, 64.2, 59.9, 56.8; ESI-MS m/z $[M+Na]^+$ calcd 261.0945, found 261.0963.

4.8. Computational methods

The Monte Carlo multiple minimum search protocol implemented in Macromodel version 8.5[29] was used to generate 50,000 conformers of **3** and **4**. These conformers were then optimized using the AMBER* force field[30] as implemented in Macromodel version 8.5 with the dielectric constant of water. All optimized conformers within 12 kcal/mol of the global minimum were saved. This process resulted in 2979 unique conformations for **3** and 1050 unique conformations for **4**. Each conformer was given a unique number beginning with 1 for the global minimum according to the energy calculated by the AMBER* force field and increasing up the energetic manifold.

Of the optimized conformers located using the AMBER* force field, all conformers within ~3.5 kcal/mol of the global minimum were then optimized at the HF/6-31G* level of theory using the Gaussian 03 software package.[31] Our previous studies[7] with similar hydroxylated septanosides had demonstrated that the gas-phase optimized geometries and relative energetics provided results that were virtually identical to those obtained with the Minnesota Gaussian Solvation Model[32] at the SM5.42/HF/6-31G* level of theory with water as a solvent. Optimization of these conformers within 3.5 kcal/mol of the global minimum using the HF/6-31G* level of theory resulted in 55 unique conformers within 10 kcal/mol of the global minimum for **3** and 48 unique conformers within 7.4 kcal/mol of the global minimum for **4**. A vibrational frequency analysis was performed on each optimized conformer at the HF/6-31G* level of theory to confirm each conformer as a true minimum on the potential energy surface. The bottom-of-the-well energies at the HF/6-31G* level of theory were used to calculate the contribution of each conformer to the Boltzmann distribution. Consideration of the zero-point vibrational energy, enthalpic and entropic corrections was done for many of the low-energy conformers, but the effects on the corresponding Boltzmann distribution were small. These other energetic values are provided in the Supplementary data, and the bottom-of-the-well energies are discussed herein.

To further analyze the relative energetics of the conformers and their contribution to the Boltzmann distribution, single-point energy calculations were performed at the B3LYP/6-311+G**//HF/6-31G* in the gas phase and with inclusion of solvation effects with the PCM[33] approximation for methanol. The bottom-of-the-well energies determined at these levels of theory were used to determine the contribution of each conformer to the Boltzmann distribution. Previously we noted that such an approach was a suitable protocol to compute the geometries and the relative energies of related septanosides as a balance of accuracy and computational expense.[7]

NMR coupling constants were determined for each unique conformer that contributed greater than 1% to the Boltzmann distribution using the Gaussian 03 software package with the Perdew and Wang 91 exchange and correlation functional with the IGLO-III basis set.[34] The one-bond $^1J_{C,H}$ and three-bond $^3J_{H,H}$ coupling constants were determined for each conformer,

and these values were then multiplied by their respective contribution to the Boltzmann distribution so as to compute an overall coupling constant across the entire conformational distribution. The sum of the Boltzmann distribution for each of the conformers was then compared against experimentally determined coupling constants to correlate the conformation of the septanose ring. Such simulations of the NMR coupling constants have been well utilized in the literature at the ab initio level as well as with DFT methods.[35]

4.9. NMR spectroscopy

NMR spectra used in the conformational analysis of **3** and **4** were recorded on 5–10 mM samples (0.75 mL) in CD_3OD. The $^3J_{H,H}$ values were measured by manual inspection of the peak splittings from ^1H NMR spectra (700 MHz). The simulation of the ^1H NMR spectra for **3** and **4** was done using NMRSim from Brüker.[36] Overlays comparing the simulated to the observed spectra are provided in the Supplementary data. The $^1J_{C,H}$ were measured by the inspection of ^{13}C-coupled HMQC spectra. These HMQC spectra for **3** and **4** are also provided in the Supplementary data.

4.10. Determination of the C6–C7 rotamer populations

Eqs. 1–3 were used to determine the rotamer populations about the C6–C7 bond by analysis of the $^3J_{H,H}$ coupling constants between H6 and H7*R* ($^3J_{H6,H7R}$) and H6 and H7*S* ($^3J_{H6,H7S}$). The coefficients for these equations were determined using Eq. 4.[37] The coefficients derived using other methods[38] were too large to fit the observed coupling constants and gave negative rotamer populations. The measured values of the H–C–C–H dihedral angles (ϕ) from the calculated low energy conformers of **1** and **2** were used to define the calculated $^3J_{H6,H7R}$ and $^3J_{H6,H7S}$ for the tg, gt, and gg rotamers.

$$J_{\text{calcd}} = J_0 \cos^2\phi - 0.28 \text{ Hz}; \quad J_0 = 9.27 \text{ for } 0^\circ = \phi = 90^\circ \quad \text{and} \quad J_0 = 10.36 \text{ for } 90^\circ = \phi = 180^\circ \tag{4}$$

Acknowledgements

Funding was provided to M.W.P. from the Petroleum Research Fund administered by the American Chemical Society, the University of Connecticut, and the National Science Foundation (CAREER CHE-0546311). C.M.H. acknowledges financial support from the National Science Foundation, and generous computational resources from the Ohio Supercomputer Center. M.P.D. gratefully acknowledges a Procter and Gamble fellowship. The authors thank BrükerBioSpin Corp., Billerica, MA, for NMR time and technical assistance in the collection of data on compounds **3** and **4**.

Supplementary data

Supplementary data associated with this article can be found, in the online version, at doi:10.1016/j.carres.2006.09.024.

References

1. Pakulski, Z. *Pol. J. Chem.* **1996**, *70*, 667–707.
2. Castro, S.; Duff, M.; Snyder, N.; Morton, M.; Kumar, C. V.; Peczuh, M. W. *Org. Biomol. Chem.* **2005**, *3*, 3869–3872.
3. Bozo, E.; Gati, T.; Demeter, A.; Kuszmann, J. *Carbohydr. Res.* **2002**, *337*, 1351–1365.
4. (a) Li, H.; Blériot, Y.; Chantereau, C.; Mallet, J.-M.; Sollogoub, M.; Zhang, Y.; Rodríguez-Garcia, E.; Vogel, P.; Jiménez-Barbero, J.; Sinay, P. *Org. Biomol. Chem.* **2004**, *2*, 1492–1499; (b) Morís-Varas, F.; Qian, X.-H.; Wong, C. H. *J. Am. Chem. Soc.* **1996**, *118*, 7647–7652; (c) Qian, X.-H.; Morís-Varas, F.; Wong, C. H. *Bioorg. Med. Chem. Lett.* **1996**, *6*, 1117–1122; (d) Andreanna, P. R.; Sanders, T.; Janczuk, A.; Warrick, J. I.; Wang, P. G. *Tetrahedron Lett.* **2002**, *43*, 6525–6528; (e) McCort, I.; Saniere, M.; Le Merrer, Y. *Tetrahedron* **2003**, *59*, 2693–2700; (f) Lohray, B. B.; Bhushan, V.; Prasuna, G.; Jayamma, Y.; Raheem, M. A.; Papireddy, P.; Umadevi, B.; Premkumar, M.; Lakshmi, N. S.; Narayanareddy, K. *Ind. J. Chem. Sec. B—Org. Chem. Med. Chem.* **1999**, *38*, 1311–1321.
5. The correlation of flexibility and biological activity of some brevetoxin/ciguatoxin model compounds has been investigated. See: Candenas, M. L.; Pinto, F. M.; Cintado, C. G.; Morales, E. Q.; Brouard, I.; Díaz, M. T.; Rico, M.; Rodríguez, E.; Rodríguez, R. M.; Pérez, R.; Pérez, R. L.; Martín, J. D. *Tetrahedron* **2002**, *58*, 1921–1942.
6. (a) Entrena, A.; Campos, J. M.; Gallo, M. A.; Espinosa, A. *Arkivoc* **2005**, *VI*, 88–108, This article can be found online at http://www.arkat-usa.org/ark/journal/2005/I06_Juaristi/1383/EJ-1383C.asp; (b) Entrena, A.; Campos, J.; Gómez, J. A.; Gallo, M. A.; Espinosa, A. *J. Org. Chem.* **1997**, *62*, 337–349.
7. DeMatteo, M.; Snyder, N. L.; Morton, M.; Baldisseri, D. M.; Hadad, C. M.; Peczuh, M. W. *J. Org. Chem.* **2005**, *70*, 24–38.
8. (a) Bocian, D. F.; Pickett, H. M.; Rounds, T. C.; Strauss, H. L. *J. Am. Chem. Soc.* **1975**, *97*, 687–695; (b) Hendrickson, J. B. *J. Am. Chem. Soc.* **1967**, *89*, 7043–7046; (c) Hendrickson, J. B. *J. Am. Chem. Soc* **1967**, *89*, 7047–7061; (d) Bocain, D. F.; Strauss, H. L. *J. Am. Chem. Soc.* **1977**, *99*, 2876–2882; (e) Favini, G. *THEOCHEM* **1983**, *93*, 139–152.
9. Espinosa, A.; Entrena, A.; Gallo, M. A.; Campos, J.; Domínguez, J. F.; Camacho, E.; Garrido, R. *J. Org. Chem.* **1990**, *55*, 6018–6023.
10. Cremer, D.; Pople, J. A. *J. Am. Chem. Soc.* **1975**, *97*, 1354–1358.
11. Stoddart, J. F. *Stereochemistry of Carbohydrates*; John Wiley and Sons: New York, 1971.

12. Houseknecht, J. B.; McCarren, P. R.; Lowary, T. L.; Hadad, C. M. *J. Am. Chem. Soc.* **2001**, *123*, 8811–8824.
13. Rao, V. S. R.; Qasba, P. K.; Balaji, P. V.; Chandrasekaran, R. *Conformation of Carbohydrates*; Harwood Academic: Amsterdam, Netherlands, 1998.
14. Castro, S.; Fyvie, W. S.; Hatcher, S.; Peczuh, M. W. *Org. Lett.* **2005**, *7*, 4709–4712.
15. Spohr, U.; Bach, M. *Can. J. Chem.* **1993**, *71*, 1943–1954.
16. Peczuh, M. W.; Synder, N. L. *Tetrahedron Lett.* **2003**, *44*, 4057–4061.
17. Peczuh, M. W.; Snyder, N. L.; Fyvie, W. S. *Carbohydr. Res.* **2004**, *339*, 1163–1171.
18. Fyvie, W. S.; Morton, M.; Peczuh, M. W. *Carbohydr. Res.* **2004**, *339*, 2363–2370.
19. (a) Friebolin, H. *Basic One- and Two-Dimensional NMR Spectroscopy* (Becconsall, J. K. transl); Wiley-VCH Verlag GmbH: Weinheim, Germany, 2005; (b) Bovey, F. A. *Nuclear Magnetic Resonance Spectroscopy*; Academic Press: New York, NY, 1969.
20. (a) Kirby, A. J. *The Anomeric Effect and Related Stereoelectronic Effects at Oxygen*; Springer: New York, 1983; (b) *Anomeric Effect. Origins and Consequences*; Szarek, W. A., Horton, D., Eds. ACS Symposia Series 87; American Chemical Society: Washington, DC, 1979; (c) Deslongchamps, P. *Stereoelectronic Effects in Organic Chemistry*; Wiley: New York, 1983; (d) *The Anomeric Effect and Associated Electronic Effects in Organic Chemistry*; Thatcher, G. R. J., Ed. ACS Symposia Series 539; American Chemical Society: Washington, DC, 1993.
21. For discussion of the anomeric effect in seven-membered rings see Ref. 31 and: (a) Désilets, S.; St-Jacques, M. *J. Am. Chem. Soc.* **1987**, *109*, 1641–1648; (b) Désilets, S.; St-Jacques, M. *Can. J. Chem.* **1992**, *70*, 2650–2658.
22. For reference, the barrier to interconversion of cyclohexane is approximately 10.8 kcal/mol. See: (a) Carey, F. A.; Sundberg, R. J. *Advanced Organic Chemistry*, 4th ed.; Kluwer Academic/Plenum: New York, NY, 2000; (b) Pickett, H. M.; Strauss, H. L. *J. Am. Chem. Soc.* **1970**, *92*, 7281–7290; (c) O'Donoghue, P.; Luthey-Schulten, Z. A. *J. Phys. Chem. B* **2000**, *104*, 10398–10405.
23. (a) Gordon, M. T.; Lowary, T. L.; Hadad, C. M. *J. Am. Chem. Soc.* **1999**, *121*, 9682–9692; (b) Gordon, M. T.; Lowary, T. L.; Hadad, C. M. *J. Org. Chem.* **2000**, *65*, 4954–4963; (c) McCarren, P. R.; Gordon, M. T.; Lowary, T. L.; Hadad, C. M. *J. Phys. Chem. A.* **2001**, *105*, 5911–5922.
24. Bock, K.; Duus, J. Ø. *J. Carbohydr. Chem.* **1994**, *13*, 51–67.
25. Serianni, A. S.; Barker, R. *Can. J. Chem.* **1979**, *57*, 3160–3167.
26. Castro, S.; Peczuh, M. W. *J. Org. Chem.* **2005**, *70*, 3312–3315.
27. Kirschner, K. N.; Woods, R. J. *Proc. Natl. Acad. Sci. U.S.A.* **2001**, *98*, 10541–10545.
28. (a) Murray, R. W.; Singh, M. *Org. Synth.* **1997**, *74*, 91–100; (b) Gilbert, M.; Ferrer, M.; Sanchez-Baeza, F.; Messeguer, A. *Tetrahedron* **1997**, *53*, 8643–8650.
29. Mohamadi, F.; Richards, N. G. J.; Guida, W. C.; Liskamp, R.; Lipton, M.; Caufield, C.; Chang, G.; Hendrickson, T.; Still, W. C. *J. Comput. Chem.* **1990**, *11*, 440–467.
30. Homans, S. W. *Biochemistry* **1990**, *29*, 9110–9118.
31. Frisch, M. J.; Trucks, G. W.; Schlegel, H. B.; Scuseria, G. E.; Robb, M. A.; Cheeseman, J. R.; Montgomery, J. A., Jr.; Vreven, T.; Kudin, K. N.; Burant, J. C.; Millam, J. M.; Iyengar, S. S.; Tomasi, J.; Barone, V.; Mennucci, B.; Cossi, M.; Scalmani, G.; Rega, N.; Pettersson, G. A.; Nakatsuji, H.; Hada, M.; Ehara, M.; Toyota, K.; Fukuda, R.; Hasegawa, J.; Ishida, M.; Nakajima, T.; Honda, Y.; Kitao, O.; Nakai, H.; Klene, M.; Li, X.; Knox, J. E.; Hratchian, H. P.; Cross, J. B.; Adamo, C.; Jaramillo, J.; Gomperts, R.; Stratmann, R. E.; Yazyev, O.; Austin, A. J.; Cammi, R.; Pomelli, C.; Ochterski, J. W.; Ayala, P. Y.; Morokuma, K.; Voth, G. A.; Salvador, P.; Dannenberg, J. J.; Zakrzewski, V. G.; Dapprich, S.; Daniels, A. D.; Strain, M. C.; Farkas, O.; Malick, D. K.; Rabuck, A. D.; Raghavachari, K.; Foresman, J. B.; Ortiz, J. V.; Cui, Q.; Baboul, A. G.; Clifford, S.; Cioslowski, J.; Stefanov, B. B.; Lui, G.; Liashenko, A.; Piskorz, P.; Komaromi, I.; Martin, R. L.; Fox, D. J.; Keith, T.; Al-Laham, M. A.; Peng, C. Y.; Nanayakkara, A.; Challacombe, M.; Gill, P. M. W.; Johnson, B.; Chen, W.; Wong, M. W.; Gonzalez, C.; Pople, J. A. *Gaussian 03, Revision B.04*; Gaussian: Pittsburgh, PA, 2003.
32. (a) Xidos, J. D.; Li, J.; Hawkins G. D.; Liotard, D. A.; Cramer, C. J.; Truhlar, D. G.; Frisch, M. J. *MN-GSM, Version 99.2*, 1999; University of Minnesota: Minneapolis, MN 55455; (b) Li, J.; Zhu, T.; Cramer, C. J.; Truhlar, D. G. *J. Phys. Chem. A* **1998**, *102*, 1820–1831; (c) Li, J.; Hawkins, G. D.; Cramer, C. J.; Truhlar, D. G. *Chem. Phys. Lett.* **1998**, *288*, 293–298; (d) Zhu, T.; Li, J.; Hawkins, G. D.; Cramer, C. J.; Truhlar, D. G. *J. Chem. Phys.* **1998**, *109*, 9117–9133; (e) Li, J.; Zhu, T.; Hawkins, G. D.; Winget, P.; Liotard, D. A.; Cramer, C. J.; Truhlar, D. G. *Theor. Chem. Acc.* **1999**, *103*, 9–63.
33. (a) Miertus, S.; Scrocco, E.; Tomasi, J. *Chem. Phys.* **1981**, *55*, 117–129; (b) Cammi, R.; Tomasi, J. *J. Comput. Chem.* **1995**, *16*, 1449–1458; (c) Tomasi, J.; Persico, M. *Chem. Rev.* **1994**, *94*, 2027–2094; (d) Cramer, C. J.; Truhlar, D. J. *Chem. Rev.* **1999**, *99*, 2161–2200.
34. (a) Perdew, J. P.; Wang, Y. *Phys. Rev. B* **1986**, *33*, 8800–8802; (b) Perdew, J. P. *Phys. Rev. B* **1986**, *33*, 8822–8826; (c) Perdew, J. P. *Phys. Rev. B* **1986**, *34*, 7406.
35. (a) *Calculation of NMR and EPR Parameters: Theory and Applications*; Kaupp, M., Bühl, M., Malkin, V. G., Eds.; Wiley-VCH: Weinheim, 2004; (b) Zhu, Y.; Pan, Q.; Thibaudeau, C.; Zhao, S.; Carmichael, I.; Serianni, A. S. *J. Org. Chem.* **2006**, *71*, 466–479; (c) Pan, Q.; Klepach, T.; Carmichael, I.; Reed, M.; Serianni, A. S. *J. Org. Chem.* **2005**, *70*, 7542–7549; (d) Klepach, T. E.; Carmichael, I.; Serianni, A. S. *J. Am. Chem. Soc.* **2005**, *127*, 9781–9793; (e) Thibaudeau, C.; Stenutz, R.; Hertz, B.; Klepach, T.; Zhao, S.; Wu, Q.; Carmichael, I.; Serianni, A. S. *J. Am. Chem. Soc.* **2004**, *126*, 15668–15685.
36. NMRSim v4.3 as part of TOPSPIN v1.3, 2005, Brüker Biospin GmbH.
37. Blackburn, B. J.; Grey, A. A.; Smith, I. C. P.; Hruska, F. E. *Can. J. Chem.* **1970**, *48*, 2866.
38. (a) Haasnoot, C. A. G.; de Leeuw, F. A. A. M.; de Leeuw, H. P. M.; Altona, C. *Recl. Trav. Chim. Pays-Bas* **1979**, *98*, 576; (b) Altona, C.; Sundaralingam, M. *J. Am. Chem. Soc.* **1973**, *95*, 2333.